Journal of South American Earth Sciences 29 (2010) 262–277

Contents lists available at ScienceDirect

Journal of South American Earth Sciences

journal homepage: www.elsevier.com/locate/jsames

Structure and tectonic history of the foreland basins of southernmost South America

Matías C. Ghiglione [a,b,*], Javier Quinteros [a,b,1], Daniel Yagupsky [b,c], Pedro Bonillo-Martínez [d], Julio Hlebszevtich [d,2], Victor A. Ramos [a,b], Gustavo Vergani [d,2], Daniel Figueroa [d], Santiago Quesada [d], y Tomás Zapata [d]

[a] Laboratorio de Tectónica Andina, Universidad de Buenos Aires, Ciudad Universitaria, C1428EHA Buenos Aires, Argentina
[b] Consejo Nacional de Investigaciones Científicas y Técnicas (CONICET), Argentina
[c] Laboratorio de Modelado Geológico (LaMoGe), Universidad de Buenos Aires, Ciudad Universitaria, C1428EHA Buenos Aires, Argentina
[d] Gerencia de Exploración, YPF S.A., Esmeralda 255, Buenos Aires, Argentina

ARTICLE INFO

Article history:
Received 4 December 2007
Accepted 19 July 2009

Keywords:
Flexural model
Structural evolution
Foreland basin system
Effective elastic thickness
Finite element numerical model

ABSTRACT

The common elements and differences of the neighboring Austral (Magallanes), Malvinas and South Malvinas (South Falkland) sedimentary basins are described and analyzed. The tectonic history of these basins involves Triassic to Jurassic crustal stretching, an ensuing Early Cretaceous thermal subsidence in the retroarc, followed by a Late Cretaceous–Paleogene compressional phase, and a Neogene to present-day deactivation of the fold–thrust belt dominated by wrench deformation. A concomitant Late Cretaceous onset of the foreland phase in the three basins and an integrated history during the Late Cretaceous–Cenozoic are proposed. The main lower Paleocene–lower Eocene initial foredeep depocenters were bounding the basement domain and are now deformed into the thin-skinned fold–thrust belts. A few extensional depocenters developed in the Austral and Malvinas basins during late Paleocene–early Eocene times due to a temporary extensional regime resulting from an acceleration in the separation rate between South America and Antarctica preceding the initial opening of the Drake Passage. These extensional depocenters were superimposed to the previous distal foredeep depocenter, postdating the initiation of the foredeep phase and the onset of compressional deformation. Another pervasive set of normal faults of Paleocene to Recent age that can be recognized throughout the basins are interpreted to be a consequence of flexural bending of the lithosphere, in agreement with a previous study from South Malvinas basin. Contractional deformation was replaced by transpressive kinematics during the Oligocene due to a major tectonic plate reorganization. Presently, while the South Malvinas basin is dominated by the transpressive uplift of its active margin with minor sediment supply, the westward basins undergo localized development of pull-apart depocenters and transpressional uplift of previous structures. The effective elastic thickness of the lithosphere for different sections of each basin is calculated using a dynamic finite element numerical model that simulates the lithospheric response to advancing tectonic load with active sedimentation.

© 2009 Elsevier Ltd. All rights reserved.

1. Introduction

The neighboring Austral (or Magallanes), Malvinas and South Malvinas (South Falkland) sedimentary basins are connected through a continuous Neogene depocenter that runs along the southern boundary of the South America plate (Figs. 1 and 2; Robbiano et al., 1996; Yrigoyen, 1989; Galeazzi, 1998). These basins share a common, although somewhat diachronous tectonic history, involving Triassic to Early Cretaceous crustal stretching and rifting, and subsequent thermal subsidence in the retroarc, followed by a Late Cretaceous–Paleogene compressional phase, and Neogene to present-day wrench deformation (Winslow, 1982; Biddle et al., 1986; Uliana et al., 1989; Platt and Philip, 1995; Kraemer, 2003). The most important petroleum system recognized so far in the region comprises Tithonian – Neocomian source rocks and reservoirs, known as the Lower Inoceramus-Springhill petroleum system (Biddle et al., 1986; Galeazzi, 1998). However, a Cenozoic productive petroleum system recognized in the Austral and Malvinas basins, with reservoir levels represented by Cenozoic sandstones located in compressional traps (Galeazzi, 1998) is being explored throughout the region (Fish, 2005; Bonillo-Martinez et al., 2006).

Although the major steps unfolding the tectonic, structural and sedimentological evolution of the Austral basin has been known

* Corresponding author. Address: Laboratorio de Tectónica Andina, Universidad de Buenos Aires, Ciudad Universitaria, C1428EHA Buenos Aires, Argentina.
E-mail address: mcghiglione@gmail.com (M.C. Ghiglione).
[1] Present address: Deutsches GeoForschungsZentrum GFZ, Telegrafenberg, 14473Potsdam, Germany.
[2] Present address: Pluspetrol S.A., Lima 339, C1073AAG Buenos Aires, Argentina.

0895-9811/$ - see front matter © 2009 Elsevier Ltd. All rights reserved.
doi:10.1016/j.jsames.2009.07.006

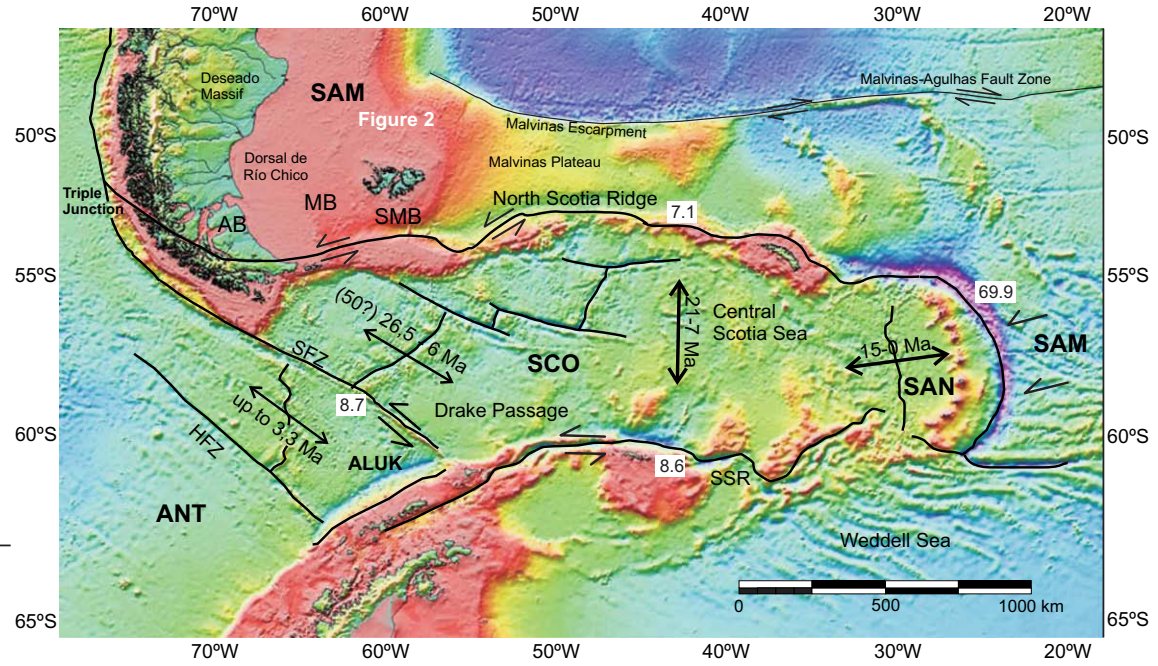

Fig. 1. Major tectonic plates enclosing the studied basins (Antarctica ANT, Sandwich SAN, Scotia SCO, South America SAM), with directions of motions at boundaries, showing velocity of plate motion relative to a fixed Scotia plate from Thomas et al. (2003), and summary of ocean floor ages and directions of opening in the Scotia Sea region from Barker (2001), Eagles et al. (2005) and Livermore et al. (2005). Abbreviations are AB: Austral basin; HFZ: Hero Fault Zone; MB: Malvinas basin; SFZ: Shackleton Fault Zone; SMB: South Malvinas basin; SSR: South Scotia Ridge. Basemap is bathymetry predicted using satellite altimetry (Sandwell and Smith, 1997).

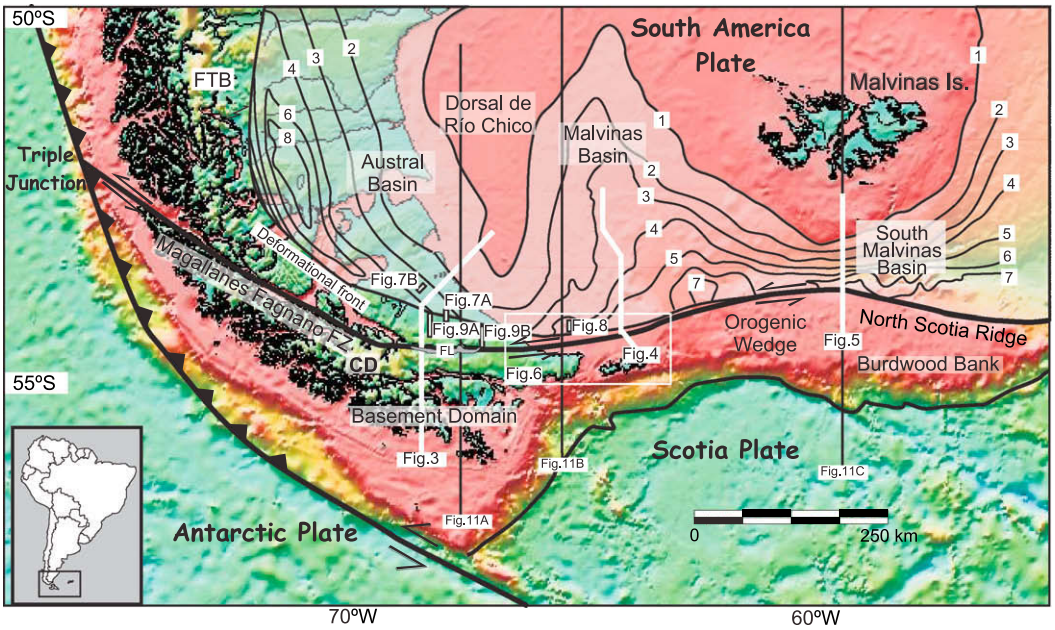

Fig. 2. Location of main morphostructural units. Contours indicate foreland sediment thickness within the undeformed depocenters in kilometers, after Ramos (1989), Galeazzi (1998) and Bry (2004) for Austral, Malvinas and South Malvinas basins respectively. Location of Figs. 4–8 and 12 are shown. Abbreviations, CD: Cordillera Darwin; FL: Fagnano Lake; FTB: fold–thrust belt, FZ: fault zone. Basemap is bathymetry predicted using satellite altimetry (Sandwell and Smith, 1997).

for more than 50 years (i.e. Thomas, 1949; Cecioni, 1957; Katz, 1963), and there also are modern studies from Malvinas (Galeazzi, 1998) and South Malvinas basins (Bry et al., 2004; Fish, 2005), modern integral analyses of these three foreland basin systems do not exist. Consequently, the main objective of the present work is to unfold the chronology of Cenozoic deformation and sedimentation of these basins. To accomplish this objective, the basins are described and examined in conjunction so as to highlight their similarities and differences. Seismic and well data from the undeformed depocenter (Biddle et al., 1986; Robbiano, 1989; Platt and Philip, 1995; Robbiano et al., 1996; Galeazzi, 1998; Bry et al., 2004; Fish, 2005; Bonillo-Martinez et al., 2006; Fig. 2) are integrated with structural and stratigraphic studies from the orogenic wedge (Olivero and Malumián, 1999, 2008; Diraison et al., 2000; Ghiglione et al., 2002; Kraemer, 2003; Yagupsky, 2003; Ghiglione and Ramos, 2005; Ghiglione et al., 2008; Tassone et al., 2005a, 2008) in order to bring forward an integrative evolution.

Data presented are integrated in a dynamical model describing the evolution of foreland basins (DeCelles and Giles, 1996; Ford, 2004) using a symptomatic approach in which sedimentary sources and depocenters migrate cratonward in response to the progressive advance of contractional deformation and tectonic load (DeCelles and Mitra, 1995; Londoño and Lorenzo, 2004). This analysis of the data allows us to challenge previous interpretations that considered the foredeep depocenter to be developed in a somewhat static location through time and helps clear up the apparent significant diachronicity in the evolution of the Austral basin when compared to the Malvinas and South Malvinas basins (e.g. Platt and Philip, 1995; Galeazzi, 1998; Bry et al., 2004).

Complementarily, the effective elastic thickness of the lithosphere is calculated using a dynamic finite element numerical model (Quinteros et al., 2006) that simulates the lithospheric response to advancing tectonic load with active sedimentation.

2. Regional setting and database

The studied basins are located at the southeastern end of the South America plate, extending across onshore southern Patagonia and Tierra del Fuego Island and the adjacent Argentine continental shelf (Figs. 1 and 2). Altogether, these basins span 1000 km from east to west and reach up to 500 km in the north–south direction (Fig. 2). Their active and uplifted boundaries are the southernmost Andes to the southwest (Wilson, 1991; Winslow, 1982; Biddle et al., 1986; Galeazzi, 1998) and the North Scotia ridge and Burdwood bank to the south (Platt and Philip, 1995; Cunningham et al., 1998; Fish, 2005; Fig. 2). The North Scotia ridge and its westward continuation, the Magallanes–Fagnano fault zone, constitute the currently active left-lateral transform boundary between South America and Scotia plates (Forsyth, 1975; Klepeis, 1994; Ramos, 1996; Barker, 2001; Figs. 1 and 2).

The studied database included 2D seismic surveys that have been acquired in the Austral basin, mostly in the onshore but also some offshore 2D seismic lines with a lower quality. Seismic surveys from Tierra del Fuego were shot mostly during the early 80s, while Austral offshore and Malvinas basins surveys were recorded mostly during late 90s. During 2005 a 2400 km^2 3D seismic survey was acquired by Repsol-YPF in the offshore Malvinas basins. Several wells have been drilled in the stable foreland basin of Malvinas and Austral basins, but so far only one well has been drilled on the offshore fold and thrust belt from Malvinas basin (Gemini). Well data include electric and mud logs, core descriptions and paleontologic reports. Synthetic seismograms and time-converted logs were used to tie seismic and well data and make lateral correlation of seismic reflectors.

3. Geological setting

Due to their location surrounded by evolving tectonic boundaries (Figs. 1 and 2), sedimentary basins from southernmost South America were not only affected by extension and rifting during Gondwana break-up (Biddle et al., 1986; Uliana and Biddle, 1987, 1988), but they were also subsequently influenced by Late Cretaceous–Paleogene Andean compressional uplift due to the interaction between the subducting oceanic plates from the Pacific basin (Farallon-Aluk-Nazca-Antarctic) and the overriding South America plate (Yrigoyen, 1989; Klepeis and Austin, 1997; Diraison et al., 2000; Somoza and Ghidella, 2005; Ghiglione and Cristallini, 2007; Ramos and Ghiglione, 2008). A recent study found evidence for a latest Paleocene–early Eocene extensional phase of continental stretching in Tierra del Fuego and its near offshore (Ghiglione et al., 2008) that coincided with a slow north-south separation of South America and Antarctica (phase I of Livermore et al., 2005).

Afterward, the region was affected by middle Eocene–Oligocene coeval strike-slip and compressional deformation due, respectively, to the fast left-lateral motion between South America and Antarctica since 50 Ma (Livermore et al., 2005), and the rapid convergence and northward-directed subduction of the Farallon plate against South America (Ramos, 2005; Ghiglione and Cristallini, 2007). This tectonic scenario impelled the onset of deformation along the Magallanes–Fagnano strike-slip fault zone producing a pervasive Neogene wrench deformation (Winslow, 1982; Klepeis, 1994; Ghiglione, 2002; Lodolo et al., 2002, 2003; Torres Carbonell et al., 2008a; Tassone et al., 2005a, 2008; Figs. 1 and 2).

The metamorphic basement of the region was generated from late Paleozoic to early Mesozoic times as an accretionary prism developed along the Pacific margin of Gondwana (Dalziel and Cortés, 1972; Dalziel, 1981; Hervé et al., 1981; Mpodozis and Ramos, 1990). The main belt of basement metamorphic rocks is located in Cordillera Darwin (Fig. 2), a high-grade metamorphic complex with up to staurolite, kyanite and sillimanite grade schist (Nelson, 1982; Dalziel, 1981; Hervé et al., 1981; Cunningham, 1995; Kohn et al., 1995). This basement is considered to be Late Paleozoic-Middle Jurassic because it reached a Rb/Sr age in whole rock of 238 ± 38 Ma (Hervé et al., 1981) and is intruded by the 164 ± 1.7 Ma old Darwin Granite Suite (Mukasa and Dalziel, 1996). The oldest basement age so far encountered was found onshore in the Austral Basin, where a granodiorite gneiss drilled in Tierra del Fuego yielded an U–Pb intrusion age in zircons of 549 ± 6 Ma (Söllner et al., 2000). Exploratory wells from the Malvinas basin found green schists intruded by granites which yielded a K–Ar age of 168 ± 3 Ma (Yrigoyen, 1989). In absence of well data, the basement from the South Malvinas basin is correlated with the Precambrian to Permian outcrops of the Malvinas Islands (Cingolani and Varela, 1976; Platt and Philip, 1995; Thomson et al., 2002; Fig. 2).

Initial subsidence began in almost all of the Patagonian hydrocarbon-producing basins during the Triassic–Jurassic continental rifting of southern South America (Uliana et al., 1989). This extensional phase continued with the opening of the Weddell Sea in Late Jurassic times and the subsequent opening of the Atlantic Ocean during the Early Cretaceous (Dalziel, 1981; Biddle et al., 1986; Ramos, 1988). The progressive stretching produced the expansion of a proto-marginal basin along the Pacific margin of the continent during Late Jurassic times (Dalziel, 1981; Mukasa and Dalziel, 1996). At least two main Jurassic extensional events are recorded in the younger graben fill of the Austral and neighboring basins of Patagonia. The early event produced a climax of extensional fault-induced subsidence in the Malvinas basin during Middle Jurassic times (Yrigoyen, 1989; Ramos, 1996; Galeazzi, 1998). The late extensional event, which was dominant in the Austral and Malvinas basin during the Late Jurassic, produced several depocenters controlled by normal faulting (Biddle et al., 1986; Robbiano, 1989; Galeazzi, 1998), filled up by an heterogeneous suite of siliceous volcanic and volcaniclastic rocks (Thomas, 1949; Yrigoyen, 1989). These rift-related Upper Jurassic heterogeneous suits of volcanic and subvolcanic rocks are called Lemaire Formation in Argentina (Caminos et al., 1981; Olivero and Martinioni, 2001) or Tobífera Formation in Chile (Thomas, 1949). In the Austral basin, these rocks are absent on some basement highs, but can reach over 2000 m in extensional depocenters (Biddle et al., 1986). Another older rift-related sedimentary succession is clearly visible in some seismic sections but its age is unknown, although it is consider as late triassic to early jurassic based on correlations with outcrops from the Patagonian Andes and the Macizo del Deseado (Biddle et al., 1986; Ramos, 1989; Yrigoyen, 1989; Fig. 1). The geometry of Mesozoic graben fill can also be recognized in seismic profiles from the South Malvinas basin, although the age and composition of their infill is estimated solely by lateral corre-

lation of seismic reflectors (Yrigoyen, 1989; Platt and Philip, 1995; Bry et al., 2004). The basement high of Dorsal de Río Chico (Dungeness arch; Zambrano and Urien, 1970; Fig. 2) probably developed during this extensional phase, separating more densely faulted depocenters from the Malvinas and Austral basins (Galeazzi, 1998). The dominant trend of the early Mesozoic rifting was mainly NW to NNW in the Austral basin (Biddle et al., 1986; Robbiano, 1989; Robbiano et al., 1996), NNW in the Malvinas basin (Yrigoyen, 1989; Galeazzi, 1998), and was predominantly E–W in the western sector of the South Malvinas basin and NE–SW in its eastern sector (Platt and Philip, 1995; Ramos, 1996).

The Upper Jurassic rift-related section is followed by an Uppermost Jurassic-Lower Cretaceous transgressive siliciclastic wedge that is represented by the Springhill and Pampa Rincón Formations (Galeazzi, 1998; Olivero and Martinioni, 2001). These retrogradational sedimentary sequences were deposited while the basins passively subsided during the sag phase characterized by minimal faulting through the Early Cretaceous (Biddle et al., 1986; Uliana et al., 1989; Ramos, 1996). The Springhill Formation is a sandstone succession of retrogradational fluvial, shoreline, and shallow-marine sandstones that represents the major hydrocarbon reservoir of the Austral and Malvinas basins (Biddle et al., 1986; Galeazzi, 1998).

The extensional regime ended in the Austral basin during Late Cretaceous times, yielding to a typical foreland phase, dominated by flexural subsidence and cratonward migration of sedimentary depocenters related to Andean uplift and expansion (Yrigoyen, 1989; Kraemer, 2003; Fildani et al., 2003; Ghiglione and Ramos, 2005; Olivero and Malumián, 2008). Late Cretaceous to Cenozoic units were derived from the south, west, and northwest, and show a progressive onlap geometry from west to east (Biddle et al., 1986). These synorogenic sequences and a series of tectonic unconformities that can be followed throughout the basins are further described in Section 4.

Previous studies suggested that the inception of the foreland phase in the Malvinas and South Malvinas basins occurred later, following a Paleocene–Middle Eocene transtensional-foredeep transitional phase (Galeazzi, 1998; Bry et al., 2004). In contrast, Fish (2005) proposed that flexural loading started as early as Late Cretaceous in the South Malvinas basin. Current works recognize the continuity between the foreland basin deposits located in the Fueguian fold and thrust belt with the Austral and Malvinas basin's undisturbed foredeep, as well as a syncronicity in the onset of their foreland phase in Late Cretaceous times (Olivero and Malumián, 1999; Ghiglione and Ramos, 2005; Torres Carbonell et al., 2008b; Lagabrielle et al., 2009; Tassone et al., 2008).

The contractional phase was replaced during Neogene times by a phase of wrench deformation induced by the fast (2.4 cm/yr) left-lateral motion between South America and Antarctica since 50 Ma (Livermore et al., 2005), producing a pervasive wrench deformation in Tierra del Fuego (Winslow, 1982; Klepeis, 1994; Ghiglione, 2002; Figs. 1 and 2).

An insight of the compressional and strike-slip phases based on new and compiled data and interpretations is presented in Section 6.

4. Morphostructure: modern and past depocenters

Five discrete and mobile tectono-stratigraphic sub-divisions can be distinguished in a foreland basin: the erosional and depositacional wedge-top, foredeep, forebulge and back-bulge depozones (DeCelles and Giles, 1996; Ford, 2004). Which depocenter a sediment particle occupies depends on its setting at the time of deposition, independently of its final position within the foreland basin. In general, the horizontal expansion of a thrust belt produces a comparable flexural wavelength in the adjacent foreland basin and an ensuing cratonward migration of depocenters (Londoño and Lorenzo, 2004), suggesting that long-term migration of the whole system should stack depocenters vertically (DeCelles and Giles, 1996). In this manner, a sedimentary sequence deposited in the forebulge depozone could eventually become buried by a foredeep sequence, and both sequences could be incorporated into the orogenic wedge afterward (e.g. the Chaco Foreland basin of southern Bolivia: Uba et al., 2006). The following descriptions include an interpretation regarding the depozone where the different sequences were deposited, allowing a broad paleobasins reconstruction.

We describe three main morphostructural units common to all of the basins (Fig. 2): (1) the orogenic wedge; (2) the undeformed foredeep depocenter; and (3) the transform plate boundary between South America and Scotia plates.

4.1. Orogenic wedge

In the present study, the orogenic wedge flanking the Austral basin is divided into three different domains from south to north (Fig. 3): (1) an internal crystalline basement-domain characterized by intense shear deformation since Late Cretaceous time (Nelson, 1982; Cunningham, 1995; Kohn et al., 1995; Klepeis and Austin, 1997; Glasser and Ghiglione, 2009); (2) an Extensional Basin Exhumation Domain, where a Jurassic-Early Cretaceous main extensional depocenter was uplifted and eroded during compressional and wrench kinematic phases; and (3) an external thin-skinned domain, formed as a result of the deformation of the Late Cretaceous–Cenozoic foreland basin infill (Figs. 2 and 3). Only the latter domain is preserved in the Malvinas basin (Fig. 4), where the basement domain drifted away during the opening of West Scotia sea.

The Burdwood bank, a 400 km wide and 160 km long block of reduced bathymetry (Fig. 2), composes the orogenic wedge from the South Malvinas basin (Fig. 5). Due to poor seismic resolution, Burdwood bank was initially interpreted to be a basement block of Paleozoic or early Mesozoic age with a narrow (~5 km) fold–thrust belt (Platt and Philip, 1995; Richards et al., 1996). Recent seismic data from Fish (2005) show that at least the southern 25 km are composed of Cenozoic foreland sediments involved in a fold–thrust belt (Fig. 5) as was previously envisaged by Dalziel and Palmer (1979).

4.2. Deformational fronts

The frontal tips of the Austral and Malvinas basin's orogenic wedges present growth structures involving pre-kinematic Eocene–Oligocene sequences and Miocene syn-kinematic strata (Figs. 7a and 8), a characteristic signature of depositional wedge-top depozones (Ford, 2004). Undeformed Pliocene to Recent sequences with a main eastward prograding trend (Bonillo-Martinez et al., 2006) cover the syn-kinematic strata in the offshore sections of these basins (Figs. 4 and 8). In contrast, the late Eocene–Miocene sequences near the deformational front of the South Malvinas basin do not show any tectonic unconformity and are covered by synorogenic Pliocene to Recent deposits (Fig. 5).

In the Austral basin, growth strata of lower Miocene age are recognized in onshore seismic sections (Fig. 7a) and outcrops in Tierra del Fuego (Ghiglione, 2002; Ghiglione and Ramos, 2005). Seismic data from onshore Tierra del Fuego show that the most external structures of the fold–thrust belt were active during Miocene times (Fig. 7a). Lower Miocene sequences outcropping along the Atlantic coast of Tierra del Fuego were deposited over active strike-slip structures, as shown by a succession of syntectonic angular and progressive unconformities, and by the presence of seismically

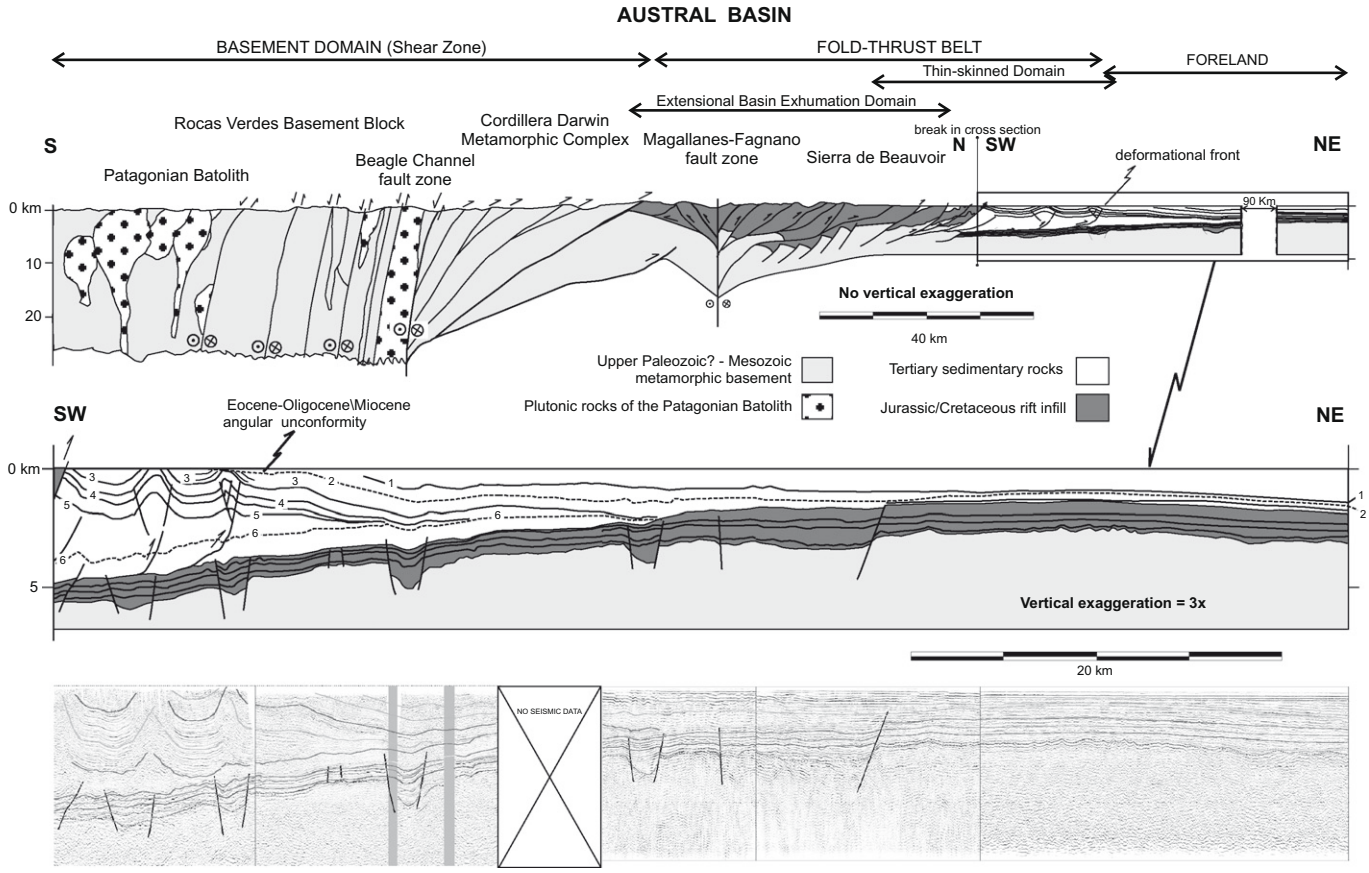

Fig. 3. Austral basin structural cross-section. Fold–thrust belt and foreland basin domains are from field data and seismic lines interpretation (shown at bottom). Basement domain is after Cunningham (1995) and Kraemer (2003). Age of stratigraphic markers is indicated by numbers as follow: 1, Miocene; 2, Eocene–Oligocene Miocene unconformity; 3, Oligocene; 4, Eocene; 5, Base of Eocene; 6, Base of Tertiary. For location, see Fig. 2.

triggered sand-intrusions (Ghiglione, 2002; Ghiglione and Ramos, 2005).

In the buried deformational front of the Malvinas fold–thrust belt, growth structures of Miocene age were covered by youngest sedimentation (Bonillo-Martinez et al., 2006). Four different evolution phases can be recognized when analyzing the geometry of sedimentary sequences through this narrow zone (Fig. 8):

(1) Overlying the tabular Cretaceous section, wedge-shaped sequences of early to middle Eocene age are truncated and incorporated into north-verging thrusts. Their south widening thickness pattern shows that, at the time of deposition, the foredeep depocenter was located southward.
(2) These sequences are covered by an upper Eocene interval. The geometry of the upper Eocene sequences shows that deposition was controlled by a set of extensional faults.
(3) These extensional faults, as well as the southern thrusts, were reversed-reactivated during the Miocene producing at least four fold-growth structures in a clearly retreating compressional setting. Indeed, while the two northern synclines concentrate the older growth strata, maximum thickness of the youngest syntectonic sequences is located in the southern synclines.
(4) Undisturbed late Neogene sequences cover the frontal structures of the fold–thrust belt. The presented seismic data shows that this Late Neogene sequences have northward-thickening geometry, and analyses of regional seismic data shows that they have a dominant sedimentary supply from the west and south (Galeazzi, 1998; Bonillo-Martinez et al., 2006).

Fish (2005) interpreted the younger sequences overlaying the deformational front in the South Malvinas basin as a post-deformational, Pliocene-Quaternary infill (Fig. 5). However, we reinterpret these sequences as synorogenic, because two synorogenic indicators characterize them: an abrupt thinning from the synclines towards the crest of the anticline and the presence of progressive unconformities (Fig. 5). The Pliocene-Quaternary sequences are overlaying an older foreland infill of late Eocene–late Miocene age that onlap against Paleocene–middle Eocene distal foredeep sequences (Fig. 5). The strong south widening thickness pattern from Paleocene to late Miocene foredeep sequences indicates that, at the time of their deposition, the main foredeep depocenter was located southward (Fig. 5).

4.3. Fold–thrust belts

The exhumed fold–thrust belt from the Austral and Malvinas basins comprises foreland basin sediments of Late Cretaceous to Miocene age (Furque and Camacho, 1949; Biddle et al., 1986; Yagupsky, 2003; Olivero and Malumián, 1999, 2008; Figs. 2–4). This exhumed fold–thrust belt of N–NE vergence can be subdivided in a southern domain with a Cretaceous decollement, and a northern domain detached within Paleocene shales (Figs. 3 and 4). One of the most striking features of the Eocene–Oligocene sedimentary sequences of the northern domain are syntectonic angular unconformities and progressive unconformities constituting growth strata (Ghiglione et al., 2002; Yagupsky, 2003; Fig. 4).

A singular characteristic of the Fueguian fold–thrust belt along the Atlantic coast is the presence of faulted detachment folds (sen-

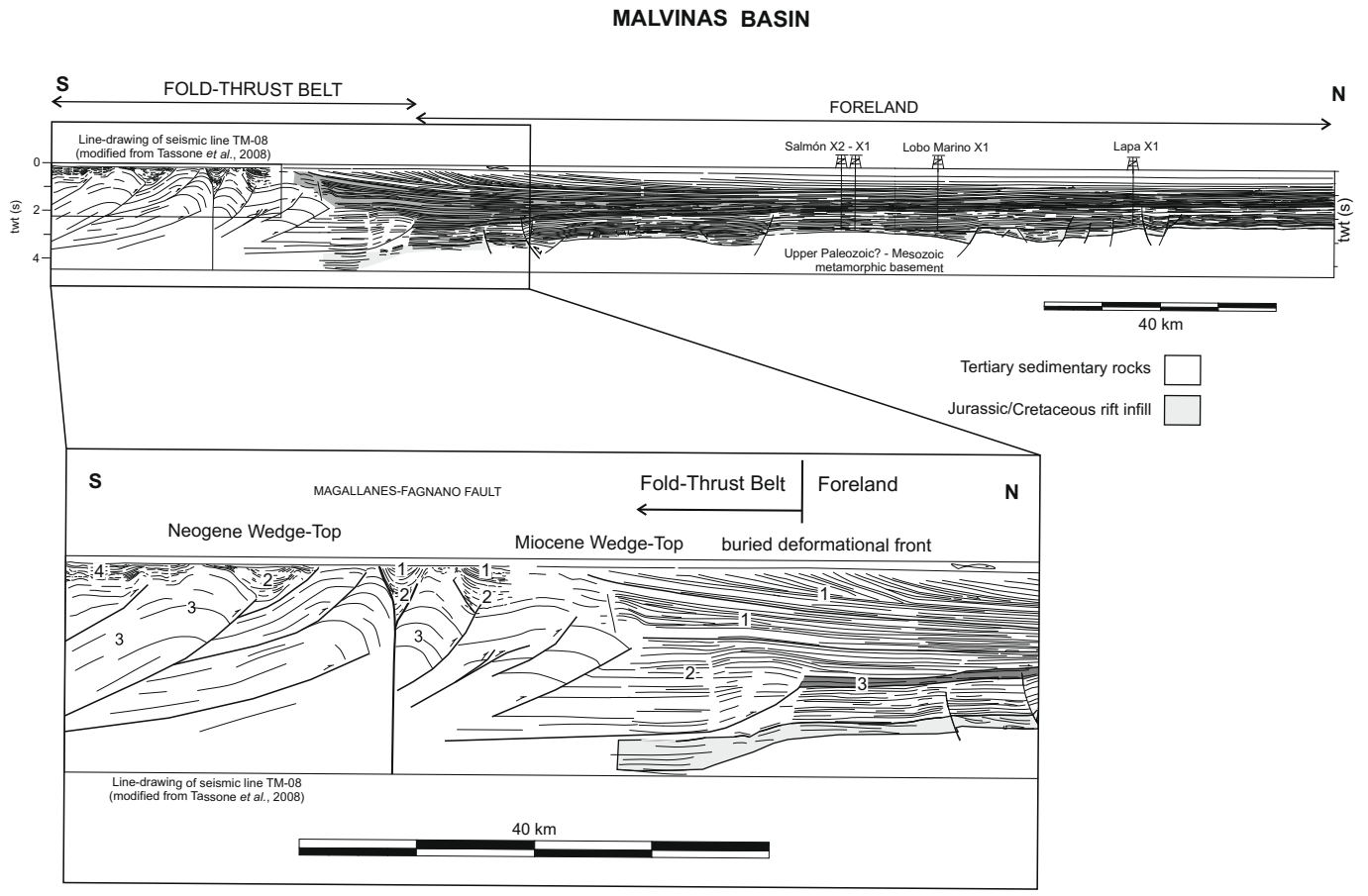

Fig. 4. Malvinas basin structural cross-section. Fold–thrust belt modified from Tassone et al. (2008), foreland basin from Galeazzi (1998). Ages of main foreland sequences are indicated by numbers as follow (after Galeazzi 1998; Tassone et al., 2008): 1, Miocene; 2, Eocene–Oligocene; 3, Late Cretaceous–Paleocene. For location, see Fig. 2.

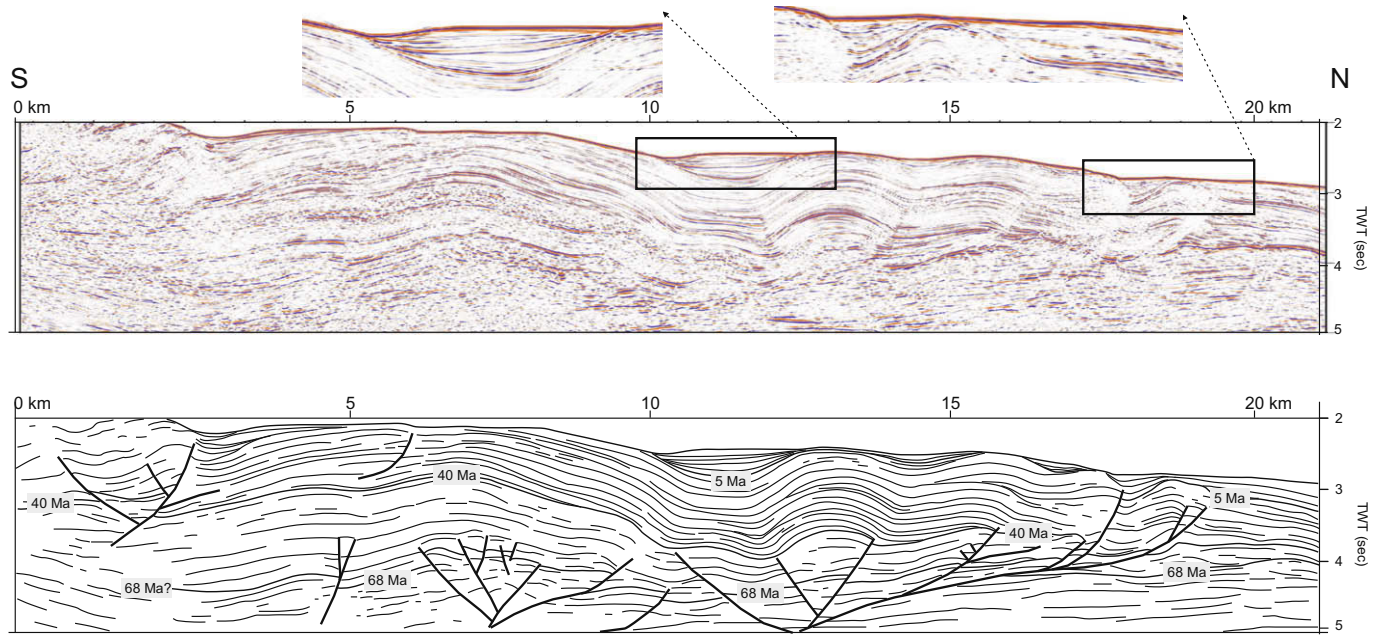

Fig. 5. South Malvinas seismic section and interpreted structural cross-sections. Original seismic sections were taken from Fish (2005) as well as stratigraphic ages. For location, see Fig. 2.

su Mitra, 2002) due to the existence of a Paleocene–early Eocene shale detachment, estimated to be around 1000 m thick, bellow a sandstone-dominated structural package (Figs. 3 and 4; Ghiglione et al., 2002). Restoration methods and kinematics forward modeling supports a folding kinematics where the folded units are characterized by strong competency contrasts and display a transition

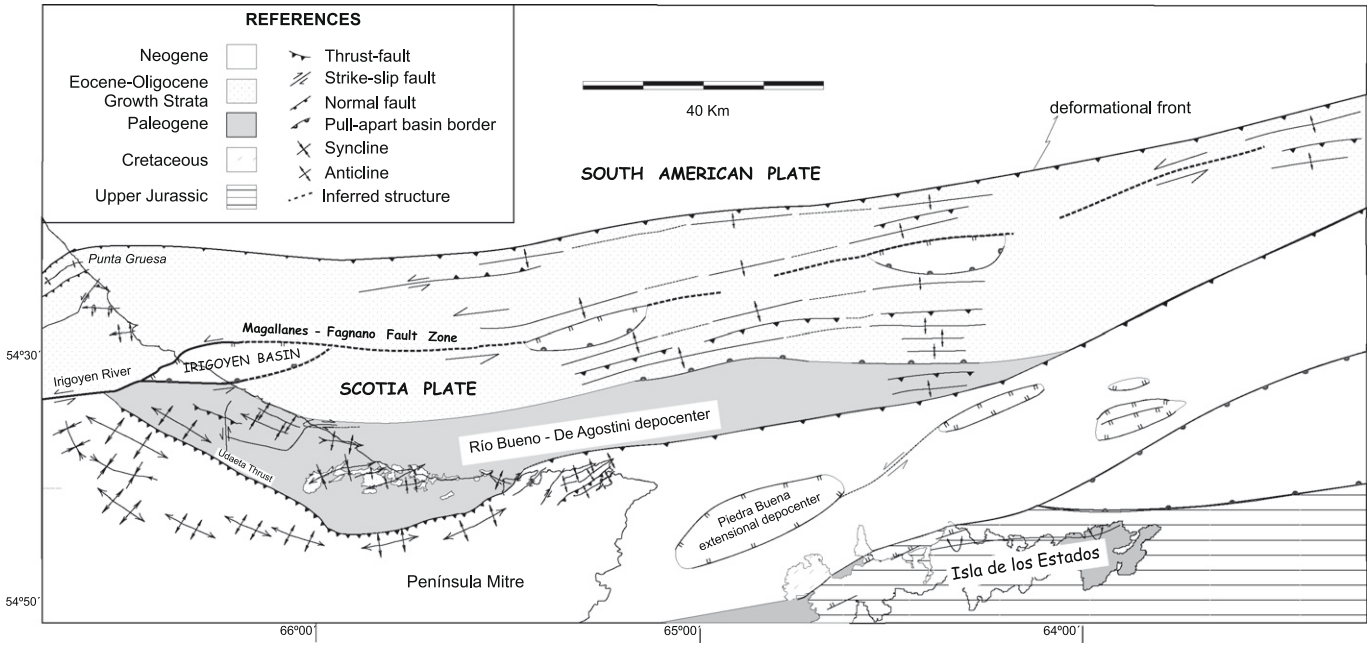

Fig. 6. Integrative Peninsula Mitre – Western Malvinas geological and structural map constructed with field data from Ghiglione (2003) and offshore seismic data from Yagupsky (2003) and Tassone et al. (2005b, 2008). For location, see Fig. 2.

in deformation behavior from detachment folding to progressive fault propagation with increasing shortening (Ghiglione et al., 2002). This strong competency contrasts means that both, the upper sandstone-dominated sequence as well as the lower mudstone detachment level played an important role (see Mitra, 2002). Recently, Torres Carbonell et al. (2008b) challenged this interpretation, stating that there are not sufficient data to prove the existence of a thick shale detachment because just the upper 450 m of this Paleocene–early Eocene sequence crops-out. However, of this 450 m, the lower 120 m are dark-gray mudstones with very few thin sandstone beds, followed by 100 m of mudstones (Olivero and Malumián, 1999, 2008), that culminate with 230 m of an heterolitic sequence dominated by 65% of mudstones (data measured from Torres Carbonell et al., 2008b). We believe that most probably, shales also dominate the not-exposed lowermost ~550 m of this distal Paleocene foredeep sequence. Although standard, palimpastically restorable fault propagation models used by Torres Carbonell et al. (2008b) can mimic the geometric structure outcropping along the Atlantic coast; they yield very unrealistic shortening rates of more than 50% and an uplift of 3.6 km in the external foothills.

However, seismic-based sections show a subtle lateral variability in the structural style of the external Fueguian fold–thrust belt with a constant 15% shortening (Bonillo-Martinez et al., 2006; Figs. 3 and 9a and b). The folds in our western sections are symmetric, display synclinal sinking, changes in bed thickness, intermediate detachment levels and have a high slip to propagation ratio (Figs. 4 and 9a) denoting a detachment mechanism for their formation. Towards the east, the anticlines are asymmetrical, northward verging, their bed thickness is maintained, and conform a fault-propagation fold geometry (Figs. 7a and 9). Further east, along the Atlantic coast, a cross-section based on a faulted detachment folds model yield around 14% (measured from Ghiglione and Ramos, 2005).

This passage from detachment folds in central Tierra del Fuego, to fault-propagation folds towards the east and faulted detachment folds along the Atlantic coast with a constant 15% shortening rate, may be denoting lateral changes in the reological properties of the detachment level. Following this reasoning, a more ductile detachment level would be present in the western (Fig. 9a) and Atlantic (Ghiglione and Ramos, 2005) sections than in the middle (Fig. 9b).

Through the northern domain flanking the Malvinas basin there is a series of piggy-back basins developing angular and progressive unconformities that can be clearly seen in seismic reflection profiles (Fig. 4). These synkinematic sequences are of Eocene to early Oligocene age, based on correlation of seismic reflectors and well data (Yagupsky, 2003; Tassone et al., 2005b, 2008). Growth strata of similar middle to late Eocene age, based on foraminifera assemblages (Olivero and Malumián, 1999), crop-out along the Atlantic coast of Tierra del Fuego (Ghiglione and Ramos, 2005). The broad extent of the middle Eocene–early Oligocene wedge-top depozone from both basins is shown in Fig. 6 by integrating seismic and field data.

In the thin-skinned Fuegian fold–thrust belt, it is possible to recognize an older syntectonic event that took place during the first steps of the Austral foreland basin. The thin-skinned external domain in Tierra del Fuego contains syntectonic angular unconformities of Uppermost Cretaceous–Lower Paleocene age constrained by dinocyst assemblage in outcrops located north of Fagnano Lake (Martinioni et al., 1999; Fig. 2) and by contents of ammonites, foraminifera, and dinocysts in Peninsula Mitre (Olivero and Martinioni, 2001; Fig. 6). These angular unconformities mark the onset of thrust propagation within foreland basin deposits, following the uplift of the internal domain (Ghiglione and Ramos, 2005). Equivalent unconformities of ~68 Ma were found within the foredeep sequences from the Malvinas and the South Malvinas basins (Bonillo-Martinez et al., 2006).

The orogenic wedge bounding the South Malvinas basin includes a northern thin-skinned domain, involving Cenozoic foreland basin deposits (Fig. 5; Fish, 2005), that is flanked to the south by an uplifted block of basement rocks (Platt and Philip, 1995; Richards et al., 1996). This deformational zone is interpreted as a continent–continent collision zone part of the North Scotia ridge, were basement is involved in the deformation (Forsyth, 1975; Ludwig and Rabinowitz, 1982; Pelayo and Wiens, 1989; Giner-Robles et al., 2003; Bry et al., 2004; Figs. 1 and 2) while shallower detachments levels are involved to the north (Fig. 5).

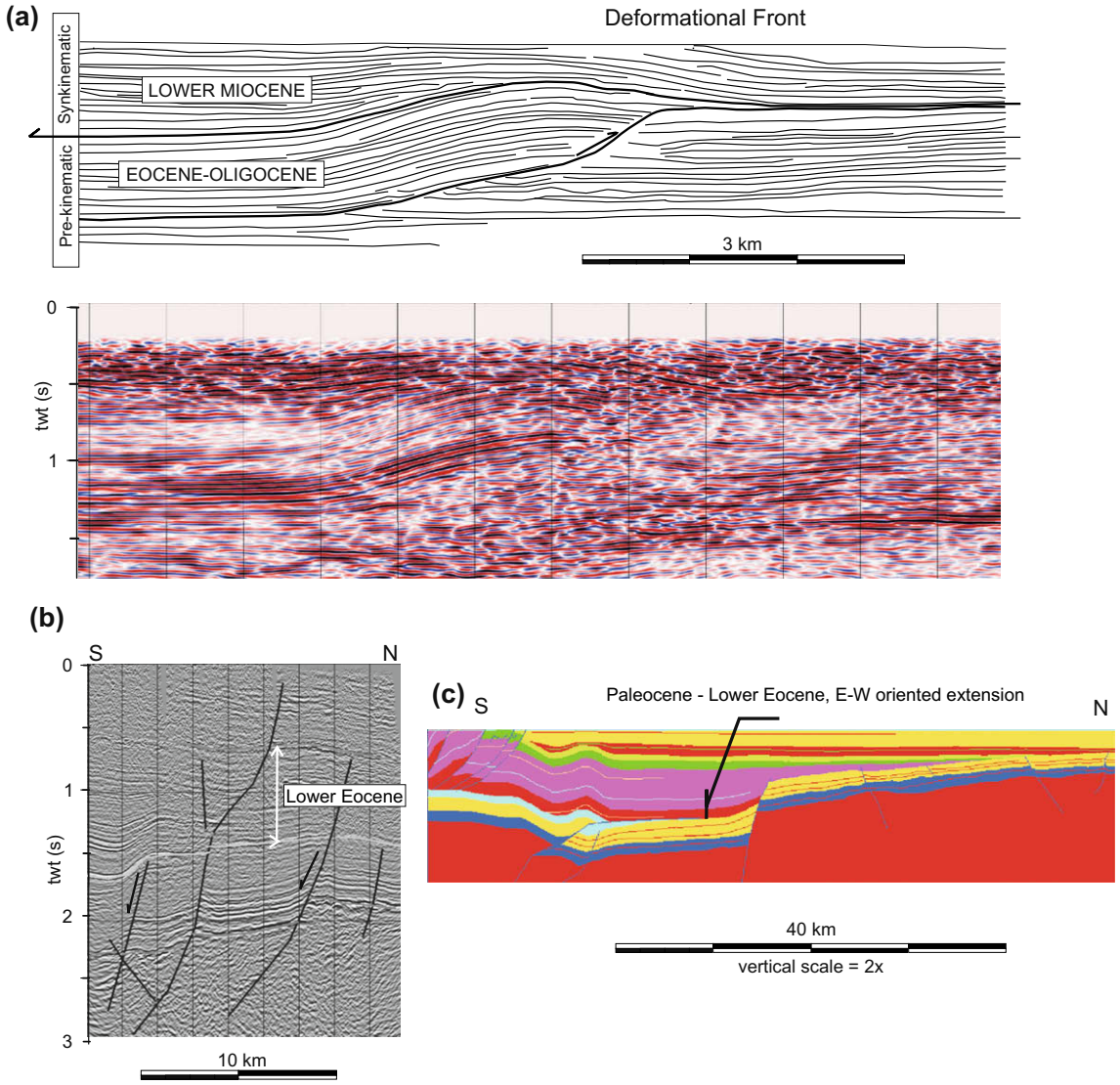

Fig. 7. Seismic data from inland Tierra del Fuego showing (a) growth strata of Lower Miocene age from the deformation front, (b) extensional growth faulting of middle Eocene age located in the undeformed depocenter, (c) transtensional faulting affecting lower Eocene sequences from offshore Austral basin. For location, see Fig. 2.

The sedimentary sequences within the thin-skinned domain of the South Malvinas basin show an overall southward widening (Fig. 5) that may suggest a zone of provenance located to the south. However, some of these sequences thin to the north and south with a double-wedge shape, implying an axial eastward-directed sedimentation, which is confirmed by extensive seismic data not shown here. A widespread erosional and angular unconformity divides the middle Eocene from the late Eocene throughout this fold–thrust belt (Fig. 5; Fish, 2005).

4.4. Undeformed foredeep depocenter

The undeformed depocenters are filled with wedge-shaped sequences thinning northward, which onlap progressively through a regional unconformity onto the previous extensional deposits (Figs. 3–5). The age of this basal foreland unconformity is Maastrichtian? in the Austral basin (Biddle et al., 1986; Robbiano, 1989; Fig. 3), but was thought to be much younger, late Eocene (~42.5 Ma) in the Malvinas basin (Galeazzi, 1998; Fig. 4), and has been tentatively dated at ~50 Ma in the South Malvinas basin by correlation with the western edge of the Malvinas basin (Bry et al., 2004). Fish (2005) proposed that the foreland basal unconformity in the South Malvinas basin is as old as Late Cretaceous on the basis of newly acquired seismic reflection data and a stratigraphic reinterpretation (Fig. 5).

In the present study, two main unconformities were found at 68 and 40 Ma, in agreement with the stratigraphic interpretation from Fish (2005). Three main unconformity-bounded sedimentary sequences overlaying the regional unconformity are recognized by correlation of seismic markers throughout the basins (Figs. 3–5 and 8; Fish, 2005):

(1) Early Paleocene–middle Eocene megasequence marked by ~68 and ~40 Ma unconformities at its base and top, respectively. This wedge-shape interval thin northward from 800 to 40–50 m. (2) Middle Eocene–late Oligocene megasequence developed on top of the ~40 Ma unconformity and covered unconformably by a progradational low late Miocene succession. The top of the sequence is an important late Miocene unconformity (5.5 Ma) covered by (3) latest Miocene–Pleistocene sequences.

The presence of extensional and strike-slip faulting in the early Paleocene–early Eocene sequences located near the deformational front (Fig. 10) lead Galeazzi (1998) to interpret this interval as a foredeep transition phase dominated by extensional and strike-slip deformation. Similar normal faulting is observed in the Austral ba-

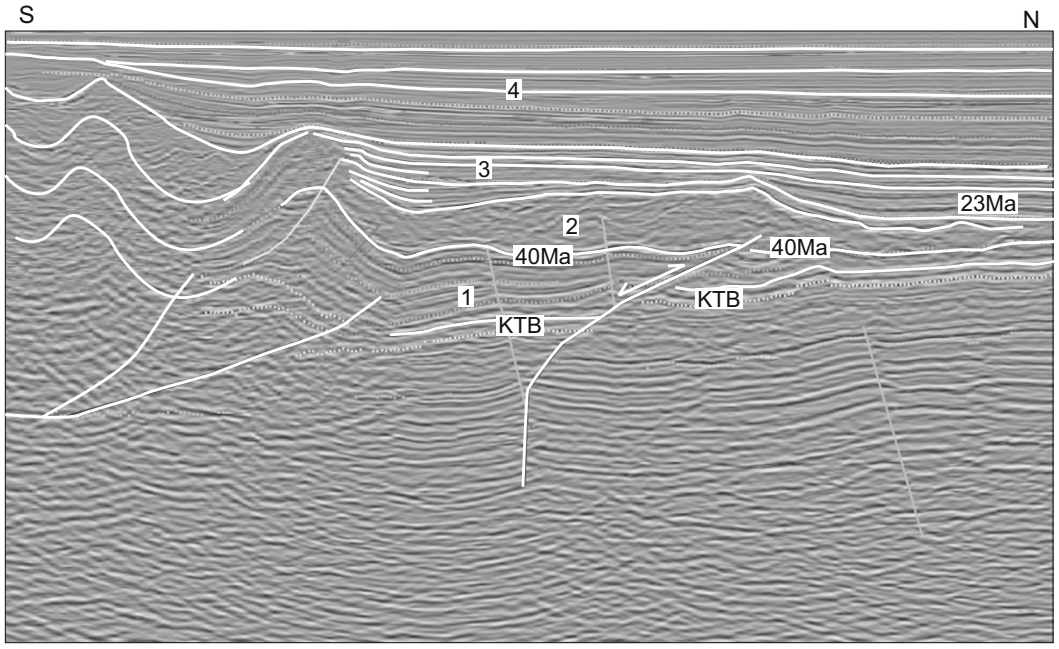

Fig. 8. Seismic data from Malvinas Basin showing geometry of extensional and compressional growth strata, see text for further discussion. Numbers indicate evolution phases discussed in text.

sin in onshore (Fig. 7b) and offshore seismic sections (Fig. 7c; see also Fig. 9 from Robbiano et al., 1996). The later are thought to be transtensive because of their en échelon distribution in map view (Bonillo-Martinez et al., 2006).

Extensional faults affecting post-sag sequences from the South Malvinas basin were previously interpreted by Platt and Philip (1995) as evidence of extensional deformation that dominated the early evolutionary stages of the foredeep. A cluster of these normal faults is concentrated ahead of the deformational front and was synchronous with the first foreland sequences, as shown by the presence of growth faulting and fault-cutting relationships (Thomson et al., 2002; Bry et al., 2004). Normal faulting extends through the flexed plate decreasing its displacement and age towards Malvinas Island. This observation led Bry et al. (2004) to suggest that normal faulting was contemporaneous with the compressional phase. These authors interpret these normal faults as flexural-related, i.e. intrinsically related to a compression-driven tectonic load and not to an overall extensional phase.

4.5. Transform plate boundary

The left-lateral plate boundary between South America and Scotia plates runs from the triple junction with the Antarctic plate in the Pacific ocean towards the Magallanes channel (Wilson, 1991; Klepeis and Austin, 1997; Figs. 1 and 2), continues through the Fagnano lake, where it is called the Magallanes–Fagnano fault zone (Klepeis, 1994), and then continues eastward to the Atlantic coast and offshore (Ghiglione 2002; Lodolo et al., 2002, 2003; Ghiglione and Ramos, 2005; Tassone et al., 2008). Along the Atlantic coast the Irigoyen pull-apart basin, active since Miocene–Pliocene times, is emplaced across the plate boundary (Ghiglione and Ramos, 2005; Malumián and Olivero, 2005; Fig. 6).

The plate boundary continues on the offshore constituting the North Scotia ridge, which offsets the Malvinas basin's fold–thrust belt and flanks the northern side of Burdwood bank, producing the transpressive uplift of this basement block (Fig. 5). Focal mechanisms from the North Scotia Ridge (Pelayo and Wiens, 1989) examined by fault population analysis show a substantial extensional component towards the continent and a compressive component on the offshore northern boundary of Burdwood bank (Giner-Robles et al., 2003; Figs. 1 and 2). Structural analysis of offshore seismic lines carried on by Lodolo et al. (2003) and Yagupsky (2003) shows that the change in kinematic behavior coincides with a flexure in the plate boundary from ENE to ESE that occurs northeast from State Island, around 63°30′W (Fig. 2). According to these authors, westward from this flexure there is a releasing bend scenario, where a series of Cenozoic pull-apart basins subside bounded by high angle normal faults (see also Klepeis and Austin, 1997; Tassone et al., 2008; Figs. 4 and 6), whereas eastward from the flexure there exists a restraining bend causing the transpressive uplift of Burdwood bank.

5. Effective elastic thickness and basin evolution

We used finite element numerical models to study the relation between effective elastic thickness (T_e) of the crust of the different basins and their evolution. The most important feature of the numerical model used here consists in the fact that it reproduces the plate deflection through time and allows assigning different T_e values to different segments of the profile based on the tectonic history or structural setting of the crust (Fig. 11). The mathematical bases of the numerical models used here are briefly described below; further details are given in Appendix 1 and Quinteros et al. (2006).

The equation describing the behavior of a beam under load can be expressed as

$$D\frac{\partial^4 w}{\partial x^4} + P\frac{\partial^2 w}{\partial x^2} = q(x)$$

being D the flexural rigidity, P the horizontal forces exerted on the plate, w the vertical deflection and $q(x)$ is the load applied at position x. The second term of this equation can here be discarded considering that horizontal forces are usually negligible in this type of geodynamical problems (Allen and Allen, 1990).

Also, as the lithosphere is overlying a mantle with fluid characteristics, the isostatic restoring force (buoyancy) should be considered. This force is proportional to the amount of material displaced

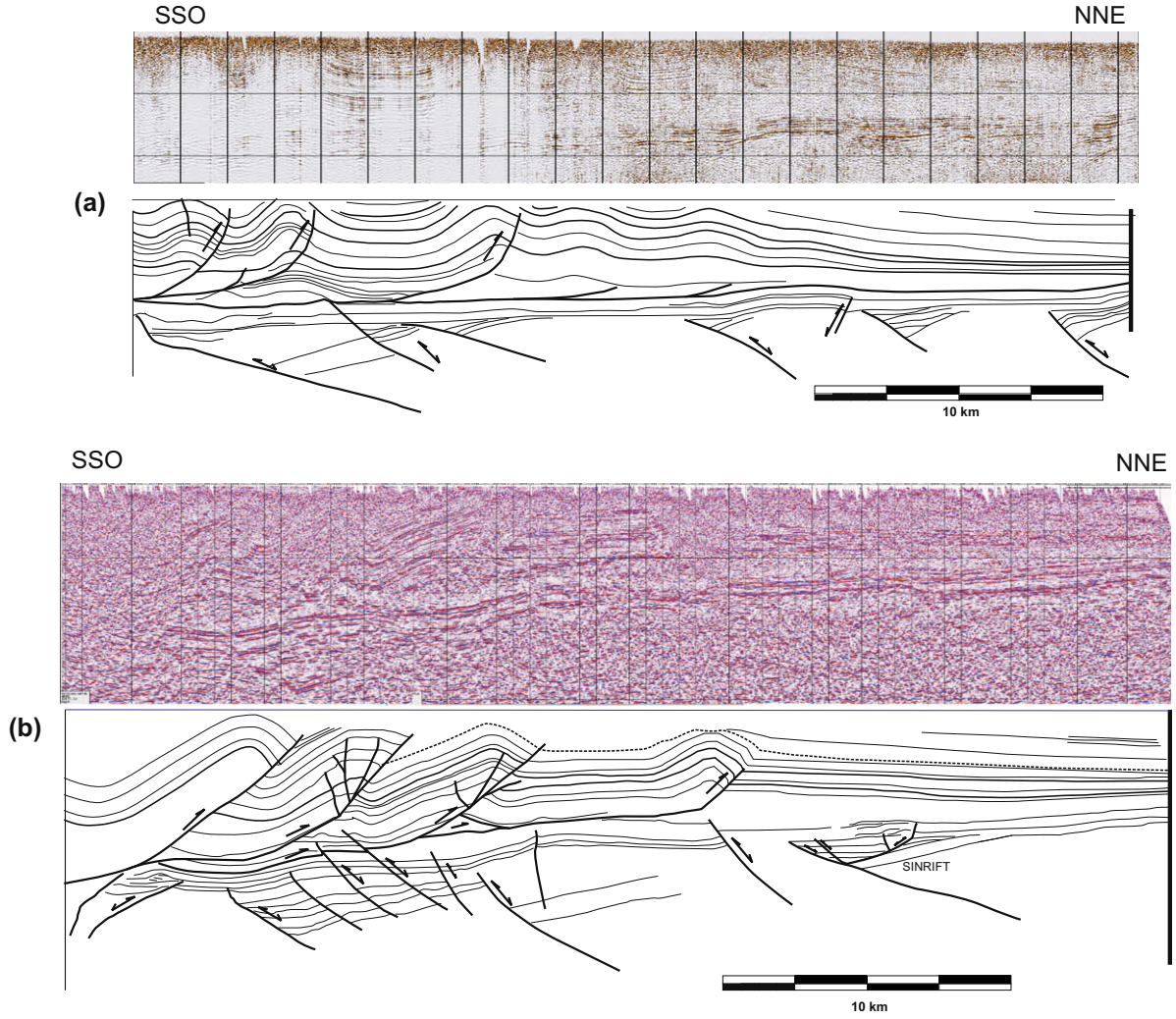

Fig. 9. Seismic data and their interpretation from inland Tierra del Fuego. See Fig. 2 for location.

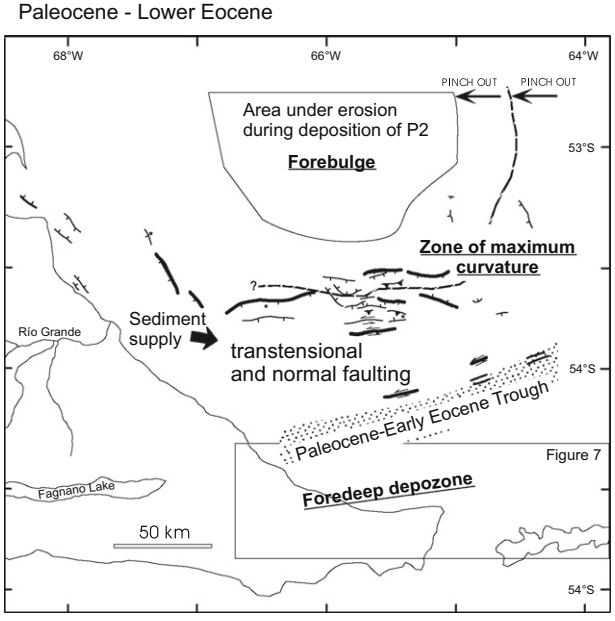

Fig. 10. Paleocene–Eocene data and paleogeography after Galeazzi (1998). Underlined text shows our reinterpretation.

beneath the crust by the bending of the lithosphere. Thus, another term is added to the equation in order to represent this situation, namely

$$D\frac{\partial^4 w}{\partial x^4} + \Delta\rho g w = q(x)$$

where $\Delta\rho$ is the density contrast between the load and the mantle, and g is the gravity acceleration.

The analytical solution for this equation exists if the flexural rigidity (D) is considered to be constant. However, it is not realistic to consider an ideal homogeneous crust. Hence, a numerical model that can include the inhomogeneities of the crust was applied.

Timoshenko's beam theory is one of the most suitable to represent the mechanical behavior of a beam. It assumes that a section of the beam that is initially normal to the neutral plane remains as a plane and with its length unchanged after deformation occurs (Timoshenko, 1934).

The density difference between the load applied and the displaced mantle is calculated taking into account how much of the deflection is filled. Namely, the density considered for the load is proportional to the infill of the deflection.

It is known that lithosphere is in a state of equilibrium whenever it is at sea level height, which means that its thickness is about 33 km (Isacks, 1988). Thus, more (or less) than this thickness shall be compensated.

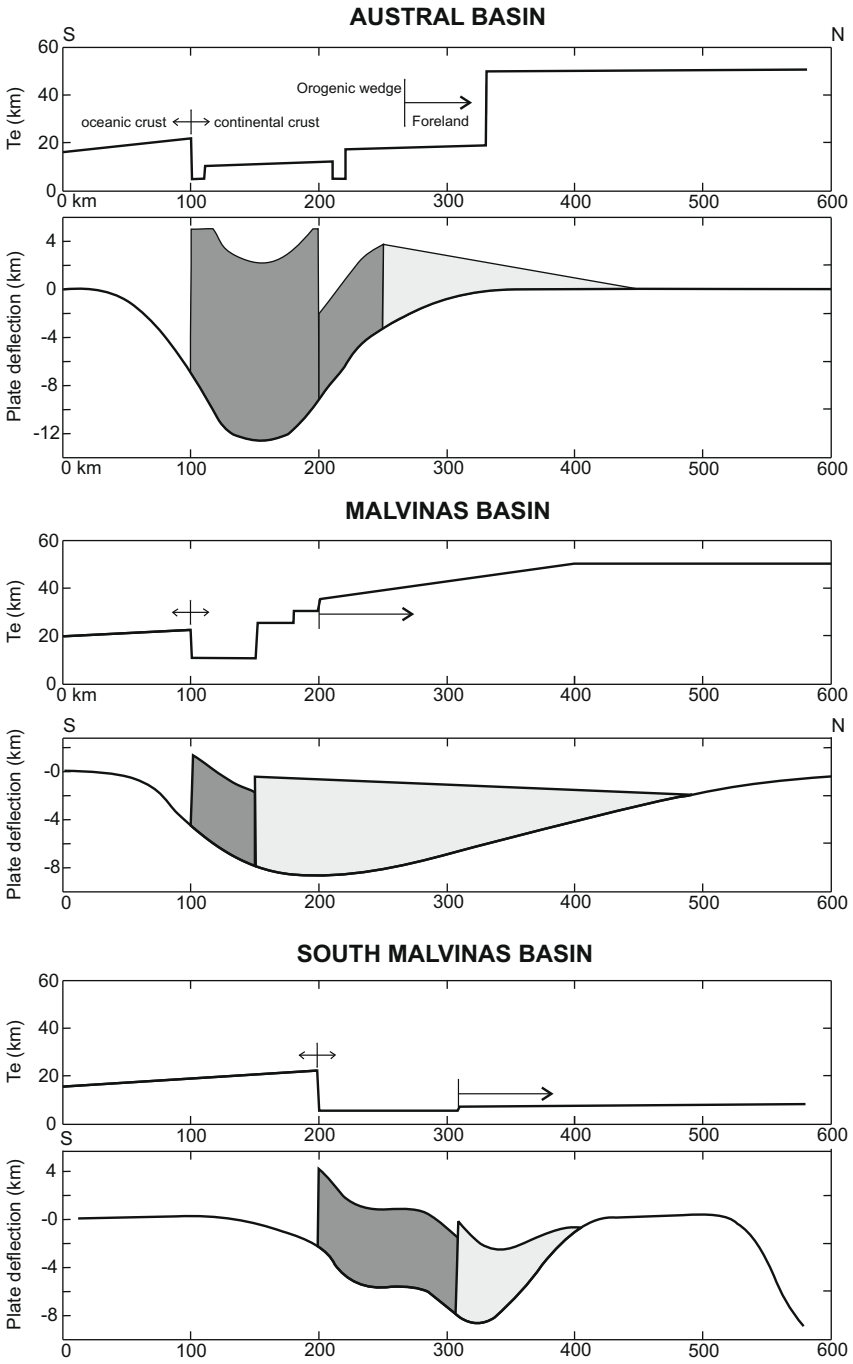

Fig. 11. Results from numerical experiments and used distribution of T_e values discussed in text. For location of plate deflection models, see Fig. 2.

The most important assumption that should be made in order to represent the crust as a beam is the election of the appropriate flexural rigidity (D). It is not a trivial decision, as the lithosphere is not homogeneous and zones of weakness can exist due to thermal anomalies or deformation processes that occurred in the past.

The flexural rigidity is usually expressed as

$$D = \frac{EaT_e^3}{12}$$

where a is the width of the beam and T_e is the effective elastic thickness. The value of this parameter has nothing to do with the real thickness of the crust or the lithosphere. It is a mechanical property related to its behavior when loaded.

5.1. Constrains on the effective elastic thickness

Previous works (see, for instance Karner et al., 1983) suggest that the most appropriate proxy for T_e is the depth at which the 450 °C isotherm is located. However, even if there is agreement about using this technique, better approximations can be obtained based on detailed studies. For instance, Bry et al. (2004) performed a very detailed gravimetric analysis to find the most accurate values in the South Malvinas basin.

The values assumed for the segments involving oceanic crust are the standard (~20 km) based on the studies of Burov and Diament (1995). For the continental crust in the South Malvinas basin, we respect the range of values of 5–7 km calculated by Bry et al. (2004). These values are the result of free-air gravity and bathym-

etry studies along several profiles in this region. The T_e values used for the Malvinas basin range from 10 to 50 km, following a westward increase in the T_e value calculated also by Bry et al. (2004). This increment seems logical, since it represents the transition from the weakened continental crust of the Malvinas plateau towards a more rigid continental crust.

In the zones where no previous studies about the strength of the lithosphere existed the values of T_e were extrapolated from well-studied zones and the values that gave the deflection profiles that were more similar to the structural sections from Figs. 3–5 were chosen.

The profile of the Austral basin includes in its northern part very high values of T_e because of the presence of the Dorsal de Rio Chico. In all the profiles, crustal discontinuities like the Magallanes–Fagnano and Beagle fault zones (Figs. 1 and 3–5) are characterized by low values of T_e due to the presence of a weak zone in the upper part of the crust because of transpression or transtensional deformation.

Fig. 11 shows the distribution of T_e values along the three selected profiles modeled from the ocean towards the continent, compare Fig. 11a–c with Figs. 3–5, respectively, to see the correlation.

Plate deflection profiles were modeled by inputting values of tectonic and sediment load calculated for each basin from its structural section (Figs. 3–5). During modeling, various values of T_e were tried and the values that gave the deflection profiles that were more similar to the structural sections from Figs. 3–5 were chosen (Fig. 11).

Uplift and sedimentation were introduced into the model as a long-term process. In this direction, small increments of the load were introduced at every time step, varying also its distribution with the resulting deflection. Restoring forces are strongly influenced by how much of the deflection is actually occupied, increasing the non-linearity of the problem. Our approach was consistent with this fact and the difference in density was calculated not only for every time step, but for every single iteration inside the time step. Despite of this, only the intermediate steps of the Austral basin model are considered for comparison with its actual evolution (Fig. 12), given that this is the only basin where the entire basement domain is preserved. Although the Magallanes–Fagnano fault system produced a displacement between the fold–thrust belt and the basement domain of up to 40 km (Winslow, 1982; Klepeis, 1994; Olivero and Martinioni, 2001; Torres Carbonell et al., 2008a); this displacement was approximately E–W and parallel to the actual boundary between both structural domains, and therefore it did not change significantly the 2D geometrical relation in our 600 km long, N–S profile from Fig. 12. On the other hand, there are large basement blocks that were once attached to Burdwood bank up to 33–40 Ma and were detached and dispersed during spreading in Drake Passage (for instance see Figs. 3 and 4 of Barker, 2001). The largest of these blocks correspond to South Georgia Island, that can be palinspastically restored immediately east of Tierra del Fuego and south of Isla de los Estados (Dalziel et al., 1981, see also Fig. 1 from Mukasa and Dalziel, 1996). Therefore, paleo-configuration of the basement domain from the Malvinas and South Malvinas basins have a great degree of uncertainty and for this reason only the last step of the model, which reproduces modern configuration, is shown.

Modeling plate deflection through time shows the cratonward migration of the sector of maximum curvature (Fig. 12), which can usually be correlated to the migration of the bulge. The early Paleocene reconstruction (62 Ma) shows that the sector of maximum curvature (distal foredeep–proximal forebulge) was located around the position of the middle Eocene–late Oligocene (50–30 Ma) proximal foredeep depocenter, i.e. the modern orogenic front (Figs. 10 and 12).

6. Discussion: an integrated tectonic history

6.1. Onset of foreland phase

Previous studies interpreted that the beginning of the compressional foreland phase started at about 42 Ma in the Malvinas basin due to the presence of normal faulting in the first post-sag megasequence located in the undeformed foredeep (Galeazzi, 1998). This author proposed the existence of a Paleocene–middle Eocene foredeep transition phase dominated by extensional and strike-slip deformation, followed by a late Eocene–Pliocene foredeep sensu stricto phase dominated by compressional deformation and full development of the Malvinas foredeep. Modern studies recognize a syncronicity in the onset of the Malvinas and Austral foreland phase during Late Cretaceous times by relating the foreland basin deposits located in the Fueguian fold and thrust belt with the Austral and Malvinas basin's undisturbed foredeep (Olivero and Malumián, 1999; Ghiglione and Ramos, 2005; Torres Carbonell et al., 2008b; Lagabrielle et al., 2009; Tassone et al., 2008).

In the South Malvinas basin, the foreland basal unconformity was interpreted to be 50 Ma old (Bry et al., 2004). This interpretation implies that the foreland stage started between 30 and 40 My later in the offshore basins than in the Austral basin, where first Andean-related deposits are of Turonian to Campanian age (Dott et al., 1982; Ramos, 1989; Fildani et al., 2003; Olivero and Malumián, 2008; Ghiglione and Ramos, 2005).

Although the presence of normal faulting in the Paleocene–early Eocene interval of the Malvinas basin's undeformed foredeep was interpreted by Galeazzi (1998) as evidence for regional extensional or transtensional tectonic regime, distribution analysis of similar faulting in the South Malvinas basin (Bry et al., 2004) shows that these are probably flexural-related normal faults due to a

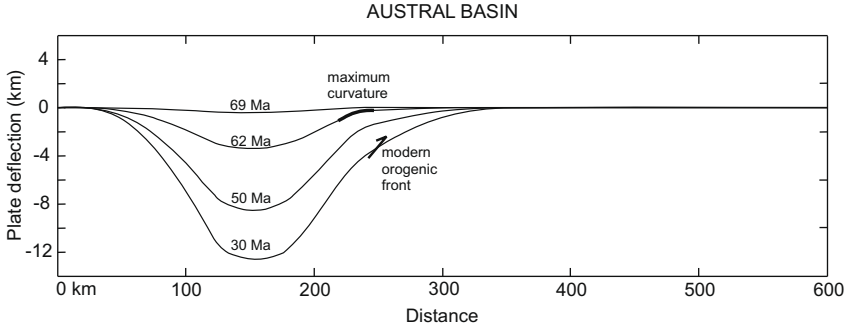

Fig. 12. 69 Ma, 62 Ma, 50 Ma and 30 Ma intermediate steps for the evolution of Austral Basin showing cratonward migration of the flexural wave. See text for discussion. See Fig. 11 for distribution of T_e values.

compression-driven tectonic load. Normal flexural-related faulting is typical of other foreland basins such as the Timor Sea basin (Londoño and Lorenzo, 2004) as well as is the onlap of sequences prograding from the foreland depocenter (Fig. 10; e.g. DeCelles and Giles, 1996). In flexural settings, the pattern of faulting is influenced by a stress distribution with fault nucleation and growth occurring preferentially in association with stress maxima along the flexural axis within the plate (see Supak et al., 2006 and references therein). Two-dimensional numerical simulations illustrate that this stress distribution results in a sequential history of fault formation, where fault nucleation is concentrated along lines of maximum bending stress aligned parallel to and at a characteristic distance from the applied load (Supak et al., 2006). Flexural modeling showing plate deflection through time shows that the zone of maximum curvature in the Austral basin during the Paleocene was located next to the modern orogenic front (Fig. 12). The Malvinas basin has a similar distribution of T_e values similar to that of the Austral basin (Fig. 11), as well as a probably similar distribution of crystalline-basement load up to Oligocene times. The position of the zone of maximum curvature through time can, therefore, be estimated to be similar in the Malvinas and Austral basins (Fig. 12).

However, the en échelon distribution in map view (Bonillo-Martinez et al., 2006) and the important displacement shown by a few of the normal faults generating small extensional depocenters located closer to the deformational front in the Malvinas basin (Figs. 7c and 8) are in agreement with the interpretation of Galeazzi (1998).

We think that these extensional depocenters are related to the early opening of Drake Passage and the first separation between South America and Antarctica at circa 50 Ma (Eagles et al., 2005; Livermore et al., 2005) which momentarily superimposed an extensional regime of widespread continental rifting over the Austral and Malvinas basins foredeep as shown by Bonillo-Martinez et al. (2006) and Ghiglione et al. (2008). Afterward, extensional faulting and stretching was concentrated southward, along the Drake Passage, due to generation of oceanic crust (Eagles et al., 2005; Livermore et al., 2005) and a mayor compressional phase affected the Fuegian Andes, driven by an orthogonal convergence vector of the Pacific/Farallon plate against South America (Ramos and Aleman, 2000; Somoza and Ghidella, 2005; Ghiglione and Cristallini, 2007). In the Río Bueno depocenter (Fig. 6), stratigraphic and tectonic relations show that the rifting was aborted a short time before the ca. 49 Ma initial deposition of basal middle Eocene carbonates (Ghiglione et al, 2008). This is in concurrence with a threefold increase in the separation rate between South America and Antarctica ca. 50 Ma, which was followed by the opening of a gap between South America and Antarctica from 50 to 34 Ma (Livermore et al., 2005). In major rift systems, the time at which crustal separation is achieved is largely a function of plate interaction and is usually preceded by a gradual reduction of tectonic activity in lateral graben systems, while tensional strain concentrates on the zone of future crustal separation (Ziegler and Cloetingh, 2004). In terms of rifting dynamics, the deactivation of Río Bueno–De Agostini depocenter (Fig. 6) as well as all the other lower Paleogene extensional depocenters (Figs. 7c and 8) can thus be explained as the abandonment of the widespread continental rift system after strain concentration on the zone of future crustal separation due to a drastic acceleration in tectonic separation.

In summary, two sets of normal faulting can be recognized:

(1) A pervasive flexural-related set due to a compression-driven tectonic load, of Paleocene to recent age.
(2) Latest Paleocene–early Eocene constrained extensional depocenters that coincide with an extensional phase of slow north-south separation of South America and Antarctica (phase I of Livermore et al., 2005).

The existence of the latter does not invalidate the presence of an older foreland stage. Furthermore, the existence of an erosional bulge cratonward from the sector affected by normal faulting in the Malvinas basin (Fig. 10) is in agreement with interpretations that the Paleocene–early Eocene trough described by Galeazzi (1998) is instead the distal foredeep, and that the main foredeep depocenter was located southward, and is now involved into the fold–thrust belt deformation (Figs. 3–5, 10 and 12). While there is extensive evidence for the location of the former Paleogene foredeep in the exhumed fold–thrust belt from the Austral basin (Biddle et al., 1986; Alvarez-Marrón et al., 1993; Olivero and Malumián, 1999, 2008; Ghiglione and Ramos, 2005; Torres Carbonell et al., 2008b; Lagabrielle et al., 2009; Tassone et al., 2008) its continuity towards the Malvinas basin fold–thrust belt can be further appreciated through integration of field and seismic data (Fig. 6).

Our cross-sections (Figs. 3–5) and map (Fig. 6) that shows a similar distribution of northward thinning Paleocene sequences, probably deposited in a proximal foredeep depozone, reveal that the three basins evolved closely together since at least earliest Cenozoic times. Although the oldest Late Cretaceous orogenic deposits and the evidence of deformation registered for the Austral basin (Ghiglione and Ramos, 2005) have not yet been found in the offshore basins due to scarce well data over the deformed zone, current data support the idea that subsidence driven by tectonic load in the offshore basins started at least during deposition of the Paleocene megasequence (Figs. 4–6).

6.2. Middle to late Eocene deformation and sedimentation

Whereas during the Paleocene–early Eocene uplift was concentrated in the basement domain (Ghiglione and Cristallini, 2007), during the middle Eocene the frontal thrust of the Austral and Malvinas basin went through a basal Paleocene shale detachment producing a rapid deformational front and depocenters migration. As discussed by Ford (2004), weak detachments cannot support any significant topography and cannot attain a critical state, producing a strong cratonward migration and expansion of the fold–thrust belt. A complementary effect found in the study zone is that the Fuegian–Malvinas fold–thrust belt stayed bellow the depositional level producing a broad wedge-top depozone (Ghiglione et al., 2002; Ghiglione and Ramos, 2005; Figs. 6).

In the South Malvinas basin, although there was a clear northward migration of deformation and depocenters, the horizontal expansion was less significant (Compare Figs. 3 and 4 with Fig. 3 from Bry et al., 2004). In this basin, the wedge-top depozone was restricted to a narrow zone and most of the Eocene sequences were deposited on a wide and thick foredeep depozone.

This contrasting geometry of broad and widely distributed wedge-top depocenters in the Austral and Malvinas basins and the presence of a narrow trough in the South Malvinas basin was also the consequence of their different T_e values. Low T_e values from the South Malvinas basin produced a short flexural wavelength when compared with the other basins (Fig. 11).

6.3. Neogene – deactivation of the fold–thrust belt and prevalence of wrench deformation

Throughout the Miocene, multiple transtensive pull-apart sedimentary depocenters appeared to affect the thin-skinned fold–thrust belt (Figs. 4 and 6; Lodolo et al., 2003; Tassone et al., 2008). We suggest that, from the lower Miocene through Recent, the subsidence concentrated in constrained depocenters was produced by the combination of previous tectonic load and pull-apart kinematics. The undeformed condition of the Pliocene sequences,

as well as an important westward provenance of sediments rather than from the southern orogen (Bonillo-Martinez et al., 2006), indicates the deactivation and burial of the Austral and Malvinas basin's fold–thrust belt (e.g. compare Figs. 3, 5 and 8 with Fig. 3c from Ford, 2004). Therefore, during the Oligocene, the cratonward migration of these fold–thrust belts stopped and compressional deformation shifted to a strike-slip offset and uplift of the previous structures. These events were related to an important tectonic plate accommodation in the Scotia arc region (Barker, 2001). More locally, they coincide with the development of the Magallanes–Fagnano fault system (Figs 1, 2 and 6). Presently, while the South Malvinas basin is dominated by the transpressive uplift of its active margin (Fig. 5), the western basins undergo localized transpressive uplift and development of pull-apart depocenters (Figs. 4 and 6). Pliocene-recent deformation in the South Malvinas basin is shown by the presence of growth strata, although they are very thin despite the available depositional space (Fig. 5). This clastic starvation is probably the consequence of the deactivation of the Fuegian Andes, and the interruption of the axial provenance of sediments that fed the South Malvinas basin during Paleogene times.

In conclusion, the eastern Austral and Malvinas basin are no longer active as foreland basins since Lower Miocene times, although they are actively deformed and affected by a wrench deformation regime.

7. Conclusions

This study highlights that, despite differences in structural styles, the basins from the southern South America plate evolved together during the foreland stage. The following main conclusions can be pointed out:

(1) A concomitant Late Cretaceous onset of foreland phase is recognized for the studied basins. The main lower Paleocene–lower Eocene initial foredeep depocenter was bounding the basement domain and is now deformed into the fold–thrust belt. Only the distal foredeep or forebulge depocenters are preserved in the modern undeformed foreland.
(2) The few extensional depocenters that developed during late Paleocene–early Eocene times northward from the present deformational front, were due to the first opening of Drake Passage. These depocenters were over-imposed to the distal foredeep depocenter of late Paleocene–early Eocene age, postdating the initiation of the foredeep stage and the onset of compressional deformation.
(3) Another pervasive set of normal faults of Paleocene to Recent age that can be recognized throughout the basins is a consequence of flexural bending of the lithosphere, in agreement with previous studies (Bry et al., 2004).
(4) Contractional deformation changed in character to wrench kinematics during the Oligocene due to major tectonic plate reorganization. Presently, while the South Malvinas basin is dominated by the transpressive uplift of its active margin with minor sediment supply, the westward basins undergo localized development of pull-apart depocenters and strike-slip offset of previous structures.

Acknowledgment

The authors want to thank REPSOL-YPF for allowing diffusion of this study. Two anonymous reviewers are also acknowledged for very thorough reviews that lead to an improved manuscript.

Appendix 1. Numerical details of the flexural model

The mechanical behavior of a beam can be expressed by means of the Timoshenko's theory. Under this theory, a section of the beam that is initially normal to the neutral plane, remains as a plane and with the same length after deformation. Because of the shear deformations, this section does not remain normal to the neutral axis. Then, the total rotation of the plane (β) is given by the rotation of the tangent to the neutral axis ($\partial w/\partial x$) and the shear deformation (γ) (Eq. (A.1)),

$$\beta = \frac{\partial w}{\partial x} - \gamma \tag{A.1}$$

being w the vertical deflection.

The deformation of a cross-section of the beam and the different angles of Eq. (A.1) can be seen in Fig. A.1.

It was already mentioned that the horizontal forces exerted on the plate P are considered negligible for this type of geodynamical problems (Allen and Allen, 1990). Then the deflection can be expressed as

$$D \cdot \frac{\partial^4 w}{\partial x^4} = q(x). \tag{A.2}$$

By the way the problem is posed, and under the assumptions of the Timoshenko's beam theory, the following variational formula can be derived from the virtual work principle:

$$E \cdot I \int_0^L \left(\frac{\partial \beta}{\partial x}\right) \cdot \delta\left(\frac{\partial \beta}{\partial x}\right) \partial x + \kappa \cdot G \cdot A \int_0^L \left(\frac{\partial w}{\partial x} - \beta\right) \cdot \delta\left(\frac{\partial w}{\partial x} - \beta\right) \partial V - \int_0^L p \cdot \delta w + m \cdot \delta\beta \, \partial x = 0 \tag{A.3}$$

where E is Young's modulus, G is the shear modulus, A is the area of the yz cross-section, p and m are the transverse and moment loading per unit length respectively and $\kappa = 5/6$ is a shear correction factor based on equating the shear strain energy yield by the constant shearing stress across the section and the actual shearing stress.

Displacements and rotations vector is defined as

$$U^T = [w_1, w_2, \ldots, w_N, \beta_1, \ldots, \beta_N] \tag{A.4}$$

where w_i is a displacement related with vertical deflection of node i, β_i is the rotation at the node and N is the number of nodes.

Then, all the usual isoparametric formulations are employed in order to interpolate, namely

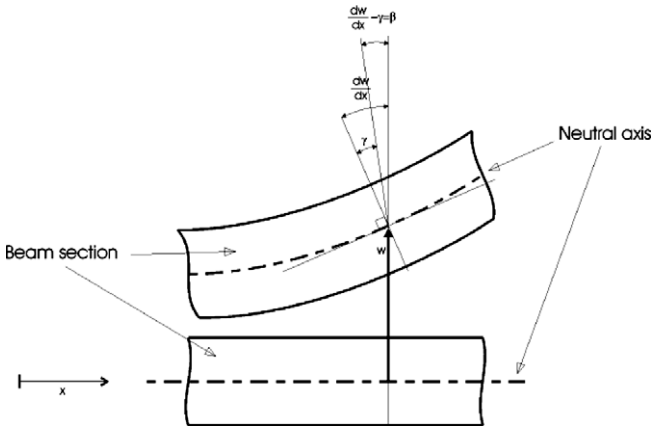

Fig. A.1. Deformation of a beam cross-section.

$$w = Hw \cdot U, \tag{A.5}$$

$$\frac{\partial w}{\partial x} = Bw \cdot U, \tag{A.6}$$

$$\beta = H_\beta \cdot U, \tag{A.7}$$

$$\frac{\partial \beta}{\partial x} = B_\beta \cdot U. \tag{A.8}$$

Replacing into Eq. (A.3) and after some algebraic steps, we get

$$\left[E \cdot I \int_0^L B_\beta^T B_\beta \, \partial x + G \cdot A \cdot \kappa \int_0^L (B_w - H_\beta)^T (B_w - H_\beta) \partial x\right] \cdot U = \int_0^L H_w^T p \, \partial x + \int_0^L H_\beta^T m \partial x. \tag{A.9}$$

The system of equations can be expressed as

$$K \cdot U = R \tag{A.10}$$

where

$$K = E \cdot I \int_0^L B_\beta^T B_\beta \, \partial x + G \cdot A \cdot \kappa \int_0^L (B_w - H_\beta)^T (B_w - H_\beta) \partial x, \tag{A.11}$$

$$R = \int_0^L H_w^T p \, \partial x + \int_0^L H_\beta^T m \, \partial x \tag{A.12}$$

and where the terms of K are related to flexure and shear stress, respectively.

But in the context of an elastic plate overlying a fluid-like mantle, isostatic restoring force (buoyancy) should be included (Turcotte and Schubert, 1982). When the material added as tectonic load above the crust cause the lithosphere to bend, material from the mantle is displaced beneath the crust. The resistance of the underlying mantle related to the load can be addressed including another term in the equation.

This way, the governing equation can be expressed as

$$D \cdot (\partial^4 w / \partial x^4) + \Delta \rho g w = q(x), \tag{A.13}$$

where $\Delta\rho$ is the density contrast between the load and the upward restoring mantle and g is the acceleration of gravity.

So, the stiffness matrix (K) is modified in order to include this term in the system of equations, namely

$$K = E \cdot I \int_0^L B_\beta^T B_\beta \partial x + G \cdot A \cdot \kappa \int_0^L (B_w - H_\beta)^T (B_w - H_\beta) \partial x + \int_0^L \Delta \rho \cdot g \cdot H_w \partial x. \tag{A.14}$$

As the formulation of this problem is non-linear, Newton–Raphson iteration scheme is applied in order to convergence to the solution.

References

Allen, H., Allen, J., 1990. Basin Analysis. Blackwell, Oxford, UK, pp. 262–281.

Alvarez-Marrón, J., McClay, K.R., Harambour, S., Rojas, L., Skarmeta, J., 1993. Geometry and evolution of the frontal part of the Magallanes foreland thrust and fold belt (Vicuna-Area), Tierra del Fuego, Southern Chile. American Association of Petroleum Geologist Bulletin 77, 1904–1921.

Barker, F., 2001. Scotia Sea regional tectonic evolution: implications for mantle flow and palaeocirculation. Earth Science Reviews 55, 1–39.

Biddle, K.T., Uliana, M.A., Mitchum, R.M., Fitzgerald, M.G., Wright, R.C., 1986. The stratigraphy and structural evolution of the central and eastern Magallanes Basin, southern South America. In: Allen, A., Homewood (Eds.), Foreland Basins, Blackwell Scientific Publications, International Association of Sedimentologist Special Publication 8, London, pp. 41–61.

Bonillo-Martinez, P., Ghiglione, M.C., Figueroa, D., 2006. Structural styles and tectonic framework of the fold and thrust belt in Tierra del Fuego and offshore Austral-Malvinas basins, Argentina. In: Simposio Bolivariano, Cartagena de Indias, pp. 1–8.

Bry, M., White, N., Singh, S., England, R., Trowell, C., 2004. Anatomy and formation of oblique continental collision: South Falkland basin. Tectonics 23, TC4011. doi: 10.1029/2002TC001482.

Burov, E.B., Diament, M., 1995. The effective elastic thickness of continental lithosphere: what does it really mean? Journal of Geophysical Research 100, 3905–3927.

Caminos, R., Haller, M., Lapido, J., Lizuain, O., Page, A., Ramos, V.A., 1981. Reconocimiento geológico de los Andes Fueguinos, Territorio Nacional de Tierra del Fuego: VIII Congreso Geológico Argentino, San Luis, pp. 759–786.

Cecioni, G., 1957. Cretaceous flysch and mollase in Departamento Ultima Esperanza. Magallanes Province, Chile. American Association of Petroleum Geologist Bulletin 41, 538–564.

Cingolani, C.A., Varela, R., 1976. Investigaciones geológicas y geocronológicas en el extremo sur de la Isla Gran Malvina, sector de Cabo Belgrano (Cabo Meredith) Islas Malvinas: VI Congreso Geológico Argentino, Bahía Blanca, pp. 457–474.

Cunningham, A.P., Barker, F., Tomlinson, J.S., 1998. Tectonics and sedimentary environments of the North Scotia Ridge region revealed by side-scan sonar. Journal of the Geological Society of London 155, 941–956.

Cunningham, W.D., 1995. Orogenesis at the southern tip of the Americas – the structural evolution of the Cordillera–Darwin metamorphic complex, Southernmost Chile. Tectonophysics 244, 197–229.

Dalziel, I.W.D., 1981. Backarc extension in the southern Andes: a review and critical reappraisal. Philosophical Transaction of the Royal Society of London 300, 319–335.

Dalziel, I.W.D., Cortés, R., 1972. Tectonic style of the southernmost Andes and the Antarctandes. In: XXIV International Geological Congress, pp. 316–327.

Dalziel, I.W.D., Palmer, K.F., 1979. Progressive deformation and orogenic uplift at the southern extremity of the Andes. Geological Society America Bulletin 90, 259–280.

DeCelles, G., Giles, K.A., 1996. Foreland basin system. Basin Research 8, 105–123.

DeCelles, G., Mitra, G., 1995. History of the Sevier orogenic wedge in terms of critical taper models, northeast Utah and southwest Wyoming. Geological Society of America Bulletin 107, 454–462.

Diraison, M., Cobbold, R., Gapais, D., Rossello, E.A., Le Corre, C., 2000. Cenozoic crustal thickening, wrenching and rifting in the foothills of the southernmost Andes. Tectonophysics 316, 91–119.

Dott, Jr., R.H., Winn, Jr., R.D., Smith, C.H.L., 1982. Relationship of late Mesozoic and early Cenozoic sedimentation to the tectonic evolution of the Southernmost Andes and Scotia Arc. In: Craddock, C. (Ed.), Antarctic Geoscience, University of Wisconsin Press, Madison, pp. 193–202.

Eagles, G., Livermore, R.A., Fairhead, J.D., Morris, P., 2005. Tectonic evolution of the west Scotia Sea. Journal of Geophysical Research 110, B02401. doi:10.1029/2004JB003154.

Fish, 2005. Frontier South, East Falkland basins reveal important exploration potential. Oil and Gas Journal 103, 34–40.

Fildani, A., Cope, T.D., Graham, S.A., Wooden, J.L., 2003. Initiation of the Magallanes foreland basin: timing of the southernmost Patagonian Andes orogeny revised by detrital zircon provenance analysis. Geology 31, 1081–1084.

Ford, M., 2004. Depositional wedge tops: interaction between low basal friction external orogenic wedges and flexural foreland basins. Basin Research 16, 361–375.

Forsyth, D.W., 1975. Fault plane solutions and tectonics of the South Atlantic and Scotia Sea. Journal of Geophysical Research 88, 1429–1443.

Furque, G., Camacho, H.H., 1949. El Cretácico superior de la costa Atlántica de Tierra del Fuego. Asociación Geológica Argentina Revista 4, 263–297.

Galeazzi, J.S., 1998. Structural and stratigraphic evolution of the western Malvinas Basin, Argentina. American Association of Petroleum Geologist Bulletin 82, 596–636.

Ghiglione, M.C., 2002. Diques clásticos asociados a deformación transcurrente en depósitos sinorogénicos del Mioceno inferior de la Cuenca Austral. Asociación Geológica Argentina Revista 57, 103–118.

Ghiglione, M.C., 2003. Estructura y evolución tectónica del Cretácico-Terciario de la costa Atlántica de Tierra del Fuego [Ph.D. thesis]. Buenos Aires, Universidad de Buenos Aires, p. 150.

Ghiglione, M.C., Ramos, V.A., Cristallini, E.O., 2002. Fueguian Andes foreland fold and thrust belt: structure and growth strata. Revista Geológica de Chile 29, 17–41.

Ghiglione, M.C., Ramos, V.A., 2005. Progression of deformation and sedimentation in the southernmost Andes. Tectonophysics 405, 25–46.

Ghiglione, M.C., Cristallini, E.O., 2007. Have the southernmost Andes been curved since Late Cretaceous times? An analog test for the Patagonian Orocline. Geology 35, 13–16.

Ghiglione, M.C., Yagupsky, D., Ghidella, M., Ramos, V.A., 2008. Continental stretching preceding the opening of the Drake Passage: evidence from Tierra del Fuego. Geology 36, 643–646.

Giner-Robles, J.L., González-Casado, J.M., Gumiel, Martín-Velázquez, S., 2003. Kinematic model of the Scotia plate (SW Atlantic Ocean). Journal of South American Earth Sciences 16, 179–191.

Glasser, N., Ghiglione, M.C., 2009. Structural, tectonic and glaciological controls on the evolution of fjord landscapes. Geomorphology 105, 291–302.

Hervé, F., Nelson, E., Kawashita, K., Suarez, M., 1981. New isotopic ages and the timing of orogenic events in the Cordillera Darwin, southernmost Chilean Andes. Earth and Planetary Sciences Letters 55, 257–265.

Isacks, B., 1988. Uplift of the Central Andes plateau and bending of the Bolivian Orocline. Journal of Geophysical Research 93, 3211–3231.

Karner, G.D., Steckler, M.S., Thorne, J.A., 1983. Long-term thermo-mechanical properties of the continental lithosphere. Nature 304, 250–253.

Katz, H.R., 1963. Revision of Cretaceous stratigraphy in Patagonian Cordillera of Ultima Esperanza, Magallanes Province, Chile. American Association of Petroleum Geologist Bulletin 47, 506–524.
Kohn, M.J., Spear, F.S., Harrison, T.M., Dalziel, I.W.D., 1995. Ar-40/Ar-39 Geochronology and P-T-T Paths from the Cordillera Darwin Metamorphic Complex, Tierra del Fuego, Chile. Journal of Metamorphic Geology 13, 251–270.
Klepeis, K.A., 1994. , The Magallanes and Deseado Fault zones – major segments of the South American Scotia Transform Plate Boundary in Southernmost South America, Tierra-Del-Fuego. Journal of Geophysical Research 99, 22001–22014.
Klepeis, K.A., Austin, J.A., 1997. Contrasting styles of superposed deformation in the southernmost Andes. Tectonics 16, 755–776.
Kraemer, E., 2003. Orogenic shortening and the origin of the Patagonian orocline (56 degrees S. Lat). Journal of South American Earth Sciences 15, 731–748.
Lagabrielle, Y., Goddéris, Y., Donnadieu, Y., Malavieille, J., Suarez, M., 2009. The tectonic history of Drake Passage and its possible impacts on global climate. Earth and Planetary Science Letters 279, 197–211.
Livermore, R., Nankivell, A., Eagles, G., Morris, P., 2005. Paleogene opening of Drake Passage. Earth and Planetary Sciences Letters 236, 459–470.
Lodolo, E., Menichetti, M., Bartole, R., Ben-Avraham, Z., Tassone, A., Lippai, H., 2002. Morphostructure of the central-eastern Tierra del Fuego Island from geological data and remote-sensing images. European Geophysical Society 2, 1–16.
Lodolo, E., Menichetti, M., Bartole, R., Ben-Avraham, Z., Tassone, A., Lippai, H., 2003. Magallanes–Fagnano continental transform fault (Tierra del Fuego, southernmost South America). Tectonics 22, 1076. doi:10.1029/2003TC001500.
Londoño, J., Lorenzo, J.M., 2004. Geodynamics of continental plate collision during late tertiary foreland basin evolution in the Timor Sea: constraints from foreland sequences, elastic flexure and normal faulting. Tectonophysics 392, 37–54.
Ludwig, W.J., Rabinowitz, P.D., 1982. The collision complex of the North Scotia Ridge. Journal of Geophysical Research 87, 3731–3740.
Malumián, N., Olivero, E.B., 2005. El Oligoceno-Plioceno marino del río Irigoyen, costa atlántica de Tierra del Fuego, Argentina: una conexión atlántico-pacífica. Revista Geológica de Chile 32, 117–129.
Martinioni, D.R., Olivero, E.B., Palamarczuk, S., 1999. Estratigrafía y discordancias del Cretácico superior – Paleoceno en la región central de Tierra del Fuego: I Simposio Paleógeno de América del Sur, Buenos Aires, pp. 7–16.
Mitra, S., 2002. Structural models of faulted detachment folds. American Association of Petroleum Geologist Bulletin 86, 1673–1694.
Mpodozis, C., Ramos, V.A., 1990. The Andes of Chile and Argentina, in Geology of the Andes and its relation to Hydrocarbon and Mineral Resources. In: Ericksen, G.E., Inochet, M.T.C., Reinemud, J.A. (Eds.), Geology of the Andes and its relation to Hydrocarbon and Mineral Resources, Earth Sciences, pp. 59–90.
Mukasa, S.B., Dalziel, I.W.D., 1996. Southernmost Andes and South Georgia Island, North Scotia Ridge: zircon U–Pb and muscovite Ar-40/Ar-39 age constraints on tectonic evolution of Southwestern Gondwanaland. Journal of South American Earth Sciences 9, 349–365.
Nelson, E.P., 1982. Post tectonic uplift of the Cordillera Darwin Orogenic Core Complex: evidence for fission track geochronology and closing temperature time relationships. Journal of Geological Society 139, 755–761.
Olivero, E.B., Malumián, N., 1999. Eocene stratigraphy of southeastern Tierra del Fuego Island, Argentina. American Association of Petroleum Geologist Bulletin 83, 295–313.
Olivero, E.B., Malumián, N., 2008. Mesozoic–Cenozoic stratigraphy of the Fuegian Andes, Argentina. Geologica Acta 6.
Olivero, E.B., Martinioni, D.R., 2001. A review of the geology of the Argentinian Fuegian Andes. Journal of South American Earth Sciences 14, 175–188.
Pelayo, A.M., Wiens, D.A., 1989. Seismotectonics and relative Plate motions in the Scotia Sea Región. Journal of Geophysical Research 94, 7293–7320.
Platt, N.H., Philip, R., 1995. Structure of the southern Falkland Islands continental shelf: initial results from new seismic data. Marine and Petroleum Geology 12, 759–771.
Quinteros, J., Jacovkis, Ramos, V.A., 2006. Evolution of the upper crustal deformation in subduction zones. Journal of Applied Mechanics 73, 984–994.
Ramos, V.A., 1988. Tectonics of the Late Proterozoic–Early Paleozoic: a collisional history of southern South America. Episodes 11, 168–174.
Ramos, V.A., 2005. Ridge collision and topography: foreland deformation in the Patagonian Andes. Tectonophysics 399, 73–86.
Ramos, V.A., 1989. Foothills structure in Northern Magallanes Basin, Argentina. American Association of Petroleum Geologist Bulletin 73, 887–903.
Ramos, V.A., 1996. Evolución Tectónica de la Plataforma Continental. In: Ramos, V.A., Turic, M.A. (Eds.), Geología y Recursos Naturales de la Plataforma Continental Argentina, Buenos Aires, pp. 385–404.
Ramos, V.A.; Aleman, A., 2000. Tectonic Evolution of the Andes. En: Tectonic evolution of South America. In: Milani, E.J., Thomaz Filho, A. (Eds.), International Geological Congress, No. 31, Río de Janeiro, pp. 635–685.
Ramos, V.A., Ghiglione, M.C., 2008. Tectonic evolution of the Patagonian Andes. In: Jorge Rabassa (Ed.), Late Cenozoic of Patagonia and Tierra del Fuego. "Developments in Quaternary Science" 11, Elsevier, pp. 57–71.
Richards, C., Gatliff, R.W., Quinn, M.F., Williamson, J.P., Fannin, N.G.T., 1996. The geological evolution of the Falkland Islands continental shelf. In: Storey, B.C., King, E.C., Livermore, R.A. (Eds.), Weddel Sea Tectonics and Gondwana Breakup. Geological Society London Special Publication 108, pp. 105–128.
Robbiano, J.A., 1989. Cuenca Austral sector costa afuera. In: Chebli, G.A., Spalletti, L.A. (Eds.), Cuencas sedimentarias Argentinas, Serie Correlación Geológica 6, Universidad Nacional del Tucumán, pp. 493–512.
Robbiano, J.A., Arbe, H., Gangui, A., 1996. Cuenca Austral Marina. In: Ramos, V.A., Turic, M.A. (Eds.), Geología y Recursos Naturales de la Plataforma Continental Argentina, Buenos Aires, pp. 323–342.
Sandwell, D.T., Smith, W.H.F., 1997. Marine gravity anomaly from Geosat and ERS-1 satellite altimetry. Journal of Geophysical Research 102 (B5), 10039–10054. doi:10.1029/96JB03223.
Somoza, R., Ghidella, M.E., 2005. Convergencia en el margen occidental de América del sur durante el Cenozoico: Subducción de Nazca, Farallon y Aluk. Asociación Geológica Argentina Revista 60, 797–809.
Söllner, F., Miller, H., Herve, M., 2000. An Early Cambrian granodiorite age from the pre-Andean basement of Tierra del Fuego (Chile): the missing link between South America and Antarctica? Journal of South American Earth Sciences 13, 163–177.
Supak, S., Bohnenstiehl, D.R., Buck, W.R., 2006. Flexing is not stretching: an analogue study of flexure-induced fault populations. Earth and Planetary Sciences Letters 246, 125–137.
Tassone, A., Lippai, H., Lodolo, E., Menichetti, M., Comba, A., Hormaechea, J.L., Vilas, J.F., 2005a. A geological and geophysical crustal section across the Magallanes–Fagnano fault in Tierra del Fuego. Journal South American Earth Sciences 19, 99–109.
Tassone, A., Yagupsky, D.L., Lodolo, E., Menichetti, M. Lippai, H., 2005b. Seismic study of the southernmost Andes in the SW Atlantic Ocean: Main wrench faults and associated basin. 6th International Symposium on Andean Geodynamics (ISAG 2005, Barcelona), Extended Abstracts: 722–725.
Tassone, A., Lodolo, E., Menichetti, M., Yagupsky, D., Caffau, M., Vilas, J.F., 2008. Seismostratigraphic and structural setting of the Malvinas Basin and its southern margin (Tierra del Fuego Atlantic offshore). Geologica Acta 6, 55–67.
Thomas, C.R., 1949. Geology and petroleum exploration in Magallanes Province, Chile. AAPG Bulletin 33, 1553–1578.
Thomas, T., Livermore, R.A., Pollitz, F., 2003. Motion of the Scotia Sea plates. Geophysical Journal International 155, 789–804.
Thomson, K., Hegarty, K.A., Marshallsea, S.J., Green, F., 2002. Thermal and tectonic evolution of the Falkland Islands: implications for hydrocarbon exploration on the adjacent offshore region. Marine and Petroleum Geology 19, 95–116.
Timoshenko, 1934. Theory of Elasticity. McGraw-Hill, New York and London.
Torres Carbonell, J., Olivero, E.B., Dimieri, L.V., 2008a. Control en la magnitud de desplazamiento de rumbo del Sistema Transformante Fagnano, Tierra del Fuego, Argentina. Revista Geológica de Chile 35, 63–79.
Torres Carbonell, J., Olivero, E.B., Dimieri, L.V., 2008b. Structure and evolution of the Fuegian Andes foreland thrust-fold belt, Tierra del Fuego, Argentina: paleogeographic implications. Journal of South American Earth Sciences 25, 417–439.
Turcotte, D.L., Schubert, G., 1982. Geodynamics: Applications of Continuum Physics to Geological Problems. Wiley, New York.
Uba, C.E., Heubeck, C., Hulka, C., 2006. Evolution of the late Cenozoic Chaco foreland basin, southern Bolivia. Basin Research 18, 145–170.
Uliana, M.A., Biddle, K.T., 1987. Permian to Late Cenozoic evolution of northern Patagonia: main tectonic events, magmatic activity and depositional trends. In: McKenzie G.D. (Ed.), Gondwana Six: Structure, Tectonics and Geophysics, Am. Geophys. U., Geophysical Monograph, vol. 40, pp. 271-286.
Uliana, M.A., Biddle, K.T., 1988. Mesozoic–Cenozoic paleogeographic and geodynamic evolution of southern South America. Revista Brasileira Geociencias 18, 172–190.
Uliana, M.A., Biddle, K.T., Cerdán, J., 1989. Mesozoic extension and the formation of argentine sedimentary basins. In: Tankard, A.J., Balkwill, H.R. (Eds.), Extensional deformation and stratigraphy of the North Atlantic margins. American Association of Petroleum Geologist Bulletin Memoir, vol. 46, pp. 599–614.
Wilson, T.J., 1991. Transition from Back-Arc to foreland basin development in the Southernmost Andes – stratigraphic record from the Ultima-Esperanza-District, Chile. Geological Society of America Bulletin 103, 98–111.
Winslow, M.A., 1982. The structural evolution of the Magallanes basin and neotectonics in the southernmost Andes. In: Craddrock, C. (Ed.), Antarctic Geosciences, Symposium on Antarctic Geology and Geophysics, University of Wisconsin Press, Madison, pp. 143–154.
Yagupsky, D.L., 2003. Estudio sismoestratigráfico y estructural del sector meridional de las cuencas de Magallanes y Malvinas, Universidad de Buenos Aires, Thesis, p. 111.
Yrigoyen, M.R., 1989. Cuenca de Malvinas. In: Chebli, G.A., Spalletti, L.A. (Eds.), Cuencas sedimentarias Argentinas, Serie Correlación Geológica 6, Universidad Nacional del Tucumán, pp. 481–491.
Zambrano, J.J., Urien, C.M., 1970. Geological outlines of the basins in southern Argentina and their offshore extension. Journal of Geophysical Research 75, 1363–1396.
Ziegler, A., Cloetingh, S., 2004. Dynamic processes controlling evolution of rifted basins. Earth Science Reviews 64, 1–50.